

# Full title: Amyotrophic lateral sclerosis transcriptomics reveals immunological effects of low-dose interleukin-2

## Short running title: Low-dose IL-2 effects in ALS

Ilaria Giovannelli<sup>[1]</sup>, Nadhim Bayatti<sup>[1]</sup>, Abigail Brown<sup>[1]</sup>, Dennis Wang<sup>[1,2]</sup>, Marius Mickunas<sup>[3]</sup>, William Camu<sup>[4]</sup>, Jean-Luc Veyrone<sup>[5]</sup>, Christine Payan<sup>[6,7]</sup>, Cecilia Garlanda<sup>[8,9]</sup>, Massimo Locati<sup>[9,10]</sup>, Raul Juntas-Morales<sup>[4]</sup>, Nicolas Pageot<sup>[4]</sup>, Andrea Malaspina<sup>[11]</sup>, Ulf Andreasson<sup>[12]</sup>, Carey Suehs<sup>[13]</sup>, Safa Saker<sup>[14]</sup>, Christophe Masseguin<sup>[15]</sup>, John de Vos<sup>[5]</sup>, Henrik Zetterberg<sup>[12,16,17,18]</sup>, Ammar Al-Chalabi<sup>[19,20]</sup>, P. Nigel Leigh<sup>[21]</sup>, Timothy Tree<sup>[3,22]</sup>, Gilbert Bensimon<sup>[6,7,23]</sup>, Paul R. Heath<sup>[1]</sup>, Pamela J Shaw<sup>[1]\*</sup> and Janine Kirby<sup>[1]\*</sup>.

### Affiliations:

[1]: Sheffield Institute for Translational Neuroscience, Department of Neuroscience, University of Sheffield, Sheffield, United Kingdom

[2]: Department of Computer Science, University of Sheffield, Sheffield, United Kingdom

[3]: Department of Immunobiology, Faculty of Life Science and Medicine, King's College London, London, United Kingdom

[4]: Clinique du Motoneurone, CHU Gui de Chaliac, University of Montpellier, France

[5]: Department of Cell and Tissue Engineering, University of Montpellier, CHU Montpellier, Montpellier, France

[6]: Department of Biostatistics, Clinical Epidemiology, Public Health and Innovation in Methodology (BESPIM), Nîmes University Hospital, Nîmes, France

[7]: Department of Pharmacology, AP-HO Sorbonne University, Pitié-Salpêtrière Hospital, 47, Bd de l'Hôpital, F-75013 Paris, France

[8]: Humanitas Clinical & Research Center - IRCCS, Milan, Italy

[9]: Humanitas University, Pieve Emanuele, Milan, Italy

[10]: Department of Medical Biotechnologies and Translational Medicine, University Milan, Milan, Italy

[11]: Neuroscience and Trauma Centre, Institute of Cell and Molecular Medicine, Department of Neuroimmunology, Barts and the London School of Medicine and Dentistry, London, United Kingdom

[12]: Department of Psychiatry & Neurochemistry, University of Gothenburg, Mölndal,

1  
2  
3 Sweden

4 [13]: Departments of Medical Information and Respiratory Diseases, University of  
5 Montpellier, CHU Montpellier, Montpellier, France

6 [14]: DNA and Cell Bank, Genethon, Evry, France

7 [15]: Delegation for Clinical Research and Innovation, Nîmes University Hospital, Nîmes,  
8 France

9 [16]: Clinical Neurochemistry Laboratory, Sahlgrenska University Hospital, Mölndal,  
10 Sweden

11 [17]: Department of Neurodegenerative Disease, UCL Institute of Neurology, Queen Square,  
12 London, UK

13 [18]: UK Dementia Research Institute at UCL, London, UK

14 [19]: Institute of Psychiatry Psychology and Neuroscience, Department of Basic and Clinical  
15 Neuroscience, King's College London, London, UK

16 [20]: Department of Neurology, King's College Hospital, London, UK

17 [21]: The Trafford Centre for Biomedical Research, Brighton and Sussex Medical School,  
18 Falmer, Brighton BN1 9RY, UK

19 [22]: NIHR Biomedical Research Centre, Guy's and St Thomas' NHS Foundation Trust and  
20 King's College London, London, United Kingdom (UK)

21 [23]: Department of Pharmacology, Sorbonne University Médecine, F-75013 Paris, France  
22 (FR)

23  
24  
25  
26  
27  
28  
29  
30  
31  
32  
33  
34  
35  
36  
37  
38  
39 \*: Joint Senior Authors

40  
41  
42  
43  
44  
45 Corresponding Author:

46 Prof Janine Kirby

47 Sheffield Institute for Translational Neuroscience, 385a Glossop Rd, Sheffield S10 2HQ, UK  
48 j.kirby@sheffield.ac.uk

## Abstract

Amyotrophic lateral sclerosis is a fatal neurodegenerative disease causing upper and lower motor neuron loss and currently no effective disease-modifying treatment is available. A pathological feature of this disease is neuroinflammation, a mechanism which involves both CNS-resident and peripheral immune system cells. Regulatory T-cells are immune-suppressive agents known to be dramatically and progressively decreased in patients with ALS. Low-dose interleukin-2 promotes regulatory T-cell expansion and was proposed as an immune-modulatory strategy for this disease. A randomized placebo-controlled pilot phase-II clinical trial called Immuno-Modulation in Amyotrophic Lateral Sclerosis (IMODALS) was carried out to test safety and activity of low-dose interleukin-2 in 36 amyotrophic lateral sclerosis patients (NCT02059759). Participants were randomized to 1MIU, 2MIU-low-dose interleukin-2 or placebo and underwent one injection daily for five days every twenty-eight days for three cycles. In this report, we describe the results of microarray gene expression profiling of trial participants' leukocyte population. We identified a dose-dependent increase in regulatory T-cell markers at the end of the treatment period. Longitudinal analysis revealed an alteration and inhibition of inflammatory pathways occurring promptly at the end of the first treatment cycle. These responses are less pronounced following the end of the third treatment cycle, although an activation of immune-regulatory pathways, involving regulatory T-cells and T helper 2 cells, was evident only after the last cycle. This indicates a cumulative effect of repeated low-dose interleukin-2 administration on regulatory T-cells. Our analysis suggested the existence of inter-individual variation amongst trial participants and we therefore classified patients into low, moderate and high-Treg-responders. NanoString profiling revealed substantial baseline differences between participant immunological transcript expression profiles with the least responsive patients showing a more inflammatory-prone phenotype at the beginning of the trial. Finally, we identified two genes in which pre-treatment expression levels correlated with the magnitude of drug responsiveness. Therefore, we proposed a two-biomarker based regression model able to predict patient Treg-response to low-dose interleukin-2. These findings and the application of this methodology could be particularly relevant for future precision medicine approaches to treat amyotrophic lateral sclerosis.

## Keywords

Amyotrophic lateral sclerosis; transcriptomics, clinical trial, low dose interleukin 2, regulatory T cells.

## Abbreviations

ALS: Amyotrophic lateral sclerosis

D: day

DEG: Differentially expressed gene

FC: Fold change

GO BP: Gene Ontology biological process

GO: Gene Ontology

IL: Interleukin

IMODALS: Immune-modulation in amyotrophic lateral sclerosis

IPA: Ingenuity pathway analysis

Ld-IL-2: Low-dose IL-2

LOOCV: Leave one out cross validation

MIU: Million international units

PCA: Principal component analysis

QC: Quality control

qRT-PCR: Quantitative real time polymerase chain reaction

R<sup>2</sup>: Coefficient of determination

REVIGO: Reduce and visualize gene ontology

RIN: RNA integrity number

RMSE: Root mean squared error

ROS: Reactive oxygen species

TAC: Transcriptome analysis console

Th: T helper

Treg: Regulatory T-cell

WBC: White blood cell

## Introduction

Amyotrophic lateral sclerosis (ALS) is a devastating neurodegenerative disease affecting upper and lower motor neurons, causing death usually within three to five years from the diagnosis.<sup>1</sup> Currently, there is no effective disease modifying treatment available. The only approved drugs are riluzole and edaravone. However, these treatments produce only modest effects on life expectancy and disability progression.<sup>2-6</sup>

ALS is considered a multifactorial disease, as a series of mechanisms are implicated in its onset and progression.<sup>7-9</sup> Amongst these, neuroinflammation, which involves both CNS-resident and peripheral immune cells, is currently of increasing interest.<sup>10</sup> Regulatory T-cells (Tregs) represent a T-cell subset with immune-regulatory properties. They suppress excessive inflammatory responses, preventing the establishment of autoimmune disorders.<sup>11</sup> Tregs were reported to be dramatically and progressively decreased in the peripheral blood of ALS patients, and these perturbations significantly correlated with disease progression and survival.<sup>12-16</sup> In particular, at early disease stages, blood CD25<sup>+</sup>FOXP3<sup>+</sup>Tregs increase in number. This is perceived as an initial protective mechanism to suppress inflammation, whilst, as disease progresses, this attempted compensatory mechanism fails and Treg counts gradually and significantly decrease. Specifically, a shift from protective Tregs/T-helper(Th)2 and anti-inflammatory (M2) microglia phenotype to the pro-inflammatory Th1/Th17 and M1 microglia has been reported.<sup>17-20</sup> Furthermore, ALS Tregs were functionally impaired and less effective at promoting immune-suppression.<sup>14, 16, 21</sup> However, evidence of pharmacological restoration of Treg immune-modulatory functions by *in vitro* culturing in the presence of interleukin (IL)-2 and rapamycin was reported.<sup>21</sup> Additionally, studies involving ALS mouse models showed that either the passive transfer of endogenous Tregs<sup>18</sup> or intraperitoneal injection of rapamycin and IL-2c (IL-2 together with its monoclonal antibody)<sup>16</sup> can efficiently expand the Treg count and prolong survival. IL-2 is crucial for the differentiation, function and survival of Treg cells.<sup>22, 23</sup> In particular, low dose IL-2 (1d-IL-2) has been shown to be safe and to promote significant Treg expansion in healthy volunteers included in a phase I clinical trial<sup>24</sup> as well as in phase I/II<sup>25-29</sup> or II<sup>30, 31</sup> studies involving patients suffering from several autoimmune disorders.

1  
2  
3 Given this background, ld-IL-2 was proposed as an immune-modulatory treatment for ALS.  
4 A randomized, placebo-controlled pilot phase-II clinical trial, Immuno-Modulation in  
5 Amyotrophic Lateral Sclerosis (IMODALS) was carried out to understand the safety and  
6 activity of ld-IL-2 in ALS patients. Thirty-six participants were recruited and randomly  
7 divided into 3 treatment arms: placebo, 1MIU and 2MIU IL-2. Ld-IL-2 appeared to be safe  
8 and well tolerated, with no serious adverse events reported.<sup>32</sup>  
9  
10  
11  
12  
13  
14

15 In this report, we examined the gene expression changes that occurred in the IMODALS  
16 cohort. In particular, the leukocyte population from participants has been transcriptionally  
17 profiled to assess differences in the response to the two treatment doses and to determine the  
18 longitudinal profile of gene expression changes throughout the trial. Consistent with the study  
19 from Camu *et al.*, we found a dose-dependent and time-dependent upregulation of Treg-  
20 specific transcripts. Moreover, a downregulation of inflammatory-related pathways was  
21 evident in response to IL-2 administration. Finally, a regression model was generated to  
22 stratify participants and to predict the Treg-response to ld-IL-2 in patients with ALS.  
23  
24  
25  
26  
27  
28  
29  
30

## 31 **Materials and methods**

### 32 **Trial design**

33  
34  
35 IMODALS (NCT02059759) is a randomized, placebo-controlled phase-IIa clinical trial  
36 (Ethical approval number=2014,09,01-ter). Thirty-six participants between 18 and 75 years  
37 of age were recruited and randomly assigned to one of three treatment arms: 1 million  
38 International Units (MIU) or 2MIU-IL-2 (Human recombinant IL-2 also known as  
39 aldesleukin or with the commercial name Proleukin®, Novartis. This will be subsequently  
40 referred to in the text as ld-IL-2) or placebo (5% glucose solution) as previously described.<sup>32</sup>  
41 Participant characteristics are summarised in Table 1. Briefly, patients received subcutaneous  
42 injections once daily for 5 days every 28 days for a total of three administration cycles. For  
43 the purpose of transcriptomic profiling, blood was taken at four timepoints: day(D)1 or  
44 baseline; D8 three days after the first injection cycle; D64 three days after the last treatment  
45 cycle; D85 24 days after the last treatment.  
46  
47  
48  
49  
50  
51  
52  
53  
54  
55  
56  
57  
58  
59  
60

## Blood collection, processing and RNA extraction

Blood samples were collected at each study visit. LeukoLOCK™ filters (Ambion™) allowed white blood cell (WBC) isolation and cells were stabilised in RNAlater (ThermoFisher Scientific). Samples were stored at -80°C and shipped in dry ice to the Sheffield Institute for Translational Neuroscience (SITraN). Total RNA was extracted using LeukoLOCK™ Total RNA isolation kit (Ambion™) according to manufacturer's instructions. RNA quantity and quality were assessed using Nanodrop ND-1000 (Thermo Scientific) and Agilent 2100 Bioanalyser (Agilent Technologies) respectively.

## Microarray preparation, normalization and quality control

Affymetrix ClariomD human microarrays (Applied Biosystem™) were produced from WBC total RNA (200ng of RNA with RNA integrity number >8) as per manufacturer's instructions (GeneChip™ WT PLUS Reagent Kit, Applied Biosystems and GeneChip™ hybridization, Wash and Stain Kit, Applied Biosystems). A total of 107 microarrays were generated: 24 arrays from samples at D1 (12 placebo and 12 2MIU-IL-2-treated patients), 23 from D8 (12 placebo and 11 2MIU-IL-2), 36 from D64 (12 placebo, 12 1MIU and 12 2MIU-IL-2) and 24 from D85 (12 placebo and 12 2MIU-IL-2). One sample from D8, C01P011 failed RNA quality control and was therefore excluded from the analysis. Microarrays were normalized using the signal space transformation robust multi-chip analysis method. Expression Console™ (Affymetrix) software was used to perform quality control (QC). All 107 microarrays passed QC and were used for downstream analysis.

## Differential expression analysis

Microarray data from D64 were analyzed using Transcriptome Analysis Console (TAC) 4.0 (Affymetrix) to identify differential expression between placebo, 1MIU-IL-2 and 2MIU-IL-2 treated patients. Gene-level analyses were performed and RefSeq annotations were used for enrichment analyses.

To accomplish complex multifactorial-designed expression analyses, the R package Limma was used.<sup>33</sup> A RefSeq filtering was applied before launching the analyses. Three differential expression tests were performed in which treated patient transcriptomes at specific time points (D8, D64 and D85) were compared to baseline levels (D1) and to the placebo group. These analyses are referred to as:  $\Delta D8$ ;  $\Delta D64$ ;  $\Delta D85$  where T indicates treated patients and P

1  
2  
3 placebo patients while numbers specify time points. Due to samples being processed at  
4 different times, two batches were recognisable in our data. For this reason, data were adjusted  
5 for batch effects including batch identifiers as variables within the Limma statistical model.  
6  
7

8 33, 34  
9

## 10 11 **Gene enrichment and pathway analysis**

12 Lists of differentially expressed genes (DEGs), previously obtained from either TAC or  
13 Limma, were inputted into Enrichr<sup>35,36</sup> to enrich for Gene Ontology Biological Process (GO  
14 BP). Long lists of altered GO BPs were produced with often redundant terms. To allow an  
15 easier interpretation of data, the software reduce and visualize gene ontology (REVIGO) was  
16 used. This grouped GO terms into clusters depending on their semantic similarity (cut-off  
17 =0.5). A GO process was then chosen as a cluster representative to recapitulate similar terms  
18  
19 <sup>37</sup>. Finally, we used Ingenuity Pathway Analysis® (IPA®) (Qiagen Inc.) and the Ingenuity  
20 Knowledge Base to retrieve significantly altered pathways in a data set allowing predictions  
21 of their activation/inhibition through the calculation of z-scores (activation: z-score > 0,  
22 inhibition: z-score <0). <sup>38</sup> DEG lists from the Limma comparisons ΔD8 and ΔD64 were  
23 submitted to IPA and analysed. Plots were generated using ggplot2 v3.2.2, gplots v3.1.1 or  
24 treemap v2.4.2 R libraries.  
25  
26  
27  
28  
29  
30  
31  
32  
33  
34  
35

## 36 **Quantitative Real Time PCR**

37 Quantitative-real-time polymerase chain reaction (qRT-PCR) was performed for microarray  
38 data validation. Four key Treg transcripts were selected: *FOXP3* (Hs.PT.58.3671186), *IL2RA*  
39 (Hs.PT.58.2187899), *CTLA4* (Hs.PT.58.3907580), *IKZF2* (Hs.PT.58.2960172) (Integrated  
40 DNA Technologies Inc.). *GAPDH* (Hs.PT.39a.22214836) was used as a reference gene as,  
41 from microarray data, its expression was stable across all time points, with no variations  
42 amongst patient groups. All the 2MIU-IL-2 and placebo patient samples from the four time  
43 points were screened. Three technical replicates were completed for each condition.  
44  
45 200ng of total RNA were retrotranscribed to cDNA using 5x qScript™ DNA Supermix  
46 (Quantobio) by incubating samples at 25°C for 5min, at 42°C for 30min and at 85°C for  
47 5min. Subsequently, cDNA was mixed with 20X predesigned PrimeTime® qPCR Assay  
48 (Integrated DNA Technologies Inc.) and 2X Luna® Universal qPCR Master Mix (New  
49 England BioLabs® Inc.). The mixture was incubated at 95°C for 3min and 40 cycles of  
50 amplification at 95°C for 10sec and 60°C for 30sec were performed using C1000 Touch™  
51  
52  
53  
54  
55  
56  
57  
58  
59  
60

Thermal cycler (Bio-Rad). Raw Ct values were retrieved using CFX Maestro™ software (Bio-Rad).  $\Delta Ct$ ,  $\Delta\Delta Ct$  and relative concentration (R) values were computed as follows:

$$\Delta Ct = Ct_{\text{gene of interest}} - Ct_{\text{reference gene}}$$

$$\Delta\Delta Ct = \Delta Ct - (\text{average } \Delta Ct_{\text{placebo sample}})$$

$$R = 2^{-\Delta\Delta Ct}$$

## NanoString

Samples from four high (Treg level at D64 > 250 cell/ul blood), four low-Treg-responders (Treg level at D64 < 150 cell/ul) and four placebo patients at D1, D8 and D64 were investigated using the NanoString platform. Patient classification is illustrated in Table 1. Briefly, 300ng of total RNA was mixed with capture and reporter probes from the auto-immune discovery panel. A hybridization period was allowed for 16 hours at 65°C. Samples were scanned using nCounter®SPRINT profiler (NanoString Technologies Inc.). The autoimmune discovery panel contains 755 mRNA targets: 740 immune-related transcripts and 15 housekeeping genes. NanoString data was analysed using nSolver™4.0 and nCounter Advanced Analysis 2.0 (NanoString Technologies Inc.). Moreover, to identify which selection of transcripts were responsible for patient group differences, data were imported into QluCore Omics Explorer (QluCore) and multigroup comparison statistical analysis was performed.

## Multiple linear regression model

To identify predictive biomarkers of the outcome of the disease, each patient's baseline expression of genes included in the nanoString panel were correlated to their Treg level at D64 (flow cytometry data)<sup>32</sup>. Pearson's correlation tests were performed with associate t-test statistics. Six biomarker candidates -*SBNO2*, *BTLA*, *CD27*, *TRAF2*, *BLNK*, *TLR9*- were selected. Given that nanoString experiments were conducted only on a selection of patients, qRT-PCRs were performed in order to obtain data at D1 from all 12 2MIU-IL-2 treated patients and on three placebo samples as controls. qRT-PCR analyses were carried out as previously described and the following primers were used: *SBNO2* (Hs.PT.58.14833003), *BTLA* (Hs.PT.58.20005939), *CD27* (Hs.PT56a.27441991), *TRAF2* (Hs.PT.583116982), *BLNK* (Hs.PT.58.1645191), *TLR9* (Hs.PT.58.40576968) (Integrated DNA Technologies

1  
2  
3 Inc.). Their averaged expression values from three technical replicates were correlated  
4 (Pearson's correlation) with their associated Treg counts at D64. Two transcripts -*TLR9* and  
5 *CD27*- were selected and a multiple linear regression model was generated using the R `lm()`  
6 function. Scatterplot3d package in R was used for 3D-plot generation. Finally, to test our  
7 model, a leave-one-out cross-validation (LOOCV) was performed using the package `caret`  
8 `v6.0.86`.  
9

### 14 **Statistical analysis**

15  
16 Differential expression analysis was performed using TAC and Limma which use F-test and  
17 Empirical Bayes statistics to retrieve significant DEGs. In both cases, p-value ( $<0.05$ ) and  
18 fold change ( $1.2 \leq FC \leq -1.2$ ) cut-offs were applied. Fisher's exact test was used for gene  
19 enrichment by Enrichr and IPA (p-value $<0.05$ ). To identify statistical differences between  
20 sample groups in qRT-PCR data, a two-way ANOVA analysis with either Tukey's or Sidak's  
21 correction for multiple comparisons was performed when analysing differences between  
22 treatment types at a single time or across different time points within the same administration  
23 regimen, respectively. Significant (p $<0.05$ ) differentially expressed nanoString transcripts  
24 were assessed using QluCore's multigroup comparison statistical analysis. Finally, the `caret`  
25 package in R was used for regression model statistics (`lm()` function, p $<0.05$ ) and LOOCV.  
26  
27  
28  
29  
30  
31  
32  
33  
34

### 35 **Data availability statement**

36  
37 Data supporting these study findings is available from the corresponding author, upon  
38 reasonable request. Array data can be found in Gene Expression Omnibus under the code  
39 GSE163560.  
40  
41  
42  
43  
44  
45

## 46 **Results**

### 50 **Dose-dependency at D64**

51  
52 Differences in patient response to the two IL-2 doses were evaluated comparing participants'  
53 gene expression at D64, when the drug reaction was hypothesized to peak. To this end,  
54 microarrays from 1MIU and 2MIU-treated patients were compared to placebo  
55 (1MIU\_vs\_Placebo and 2MIU\_vs\_Placebo analyses) using TAC software. Following  
56 treatment with 1MIU-IL-2, 3873 transcripts (760 RefSeq-annotated) were significantly  
57  
58  
59  
60

1  
2  
3 differentially expressed (2097 decreased, 1776 increased). The 2MIU\_vs\_Placebo  
4 comparison identified 6352 significantly differentially expressed transcripts (3530 decreased,  
5 2822 increased), of which 1764 were RefSeq. Of importance, 1160 transcripts (375 RefSeq-  
6 annotated), were commonly differentially expressed (figure 1A).  
7  
8  
9

10  
11 To investigate the biological functions of the differentially expressed genes (DEGs), gene  
12 ontology analyses were performed importing RefSeq lists into Enrichr. Sixty-two GO  
13 biological processes (BPs) were found to be significantly enriched in the unique list of DEGs  
14 characteristic of 1MIU\_vs\_Placebo, which were summarised into 27 clusters using REVIGO.  
15 In contrast, transcripts exclusively differentially expressed in 2MIU\_vs\_Placebo comparison  
16 were enriched in 129 GO BPs which formed 35 REVIGO clusters. Only a few immune-  
17 related processes were identified amongst 1MIU\_vs\_placebo unique list, whereas, evidence  
18 of immune-modulation (including regulation of T and B-cell receptors and regulation of  
19 antigen receptor mediated signaling) was identified amongst the 2MIU\_vs\_placebo-exclusive  
20 list (figure 1A and supplementary figure 1). Importantly, 138 GO BPs were significantly  
21 enriched from the list of commonly DEGs in both comparisons (summarised in 26 REVIGO  
22 clusters). Interestingly, the large majority of these clusters were involved in immune-  
23 modulation: an extensive T-cell-subset regulation was reported together with modulation of  
24 production and secretion of multiple cytokines (supplementary figure 1). This suggested that  
25 both doses were possibly able to promote Treg expansion and/or activation. Interestingly,  
26 transcripts involved in ganglioside and lipid metabolism were also reported as commonly  
27 altered (upregulated) following the administration of both 1d-IL-2 doses (supplementary  
28 figure 1).  
29  
30  
31  
32  
33  
34  
35  
36  
37  
38  
39  
40  
41  
42

43 To investigate potential differences in the magnitude of Treg activation, fold changes from  
44 the two comparisons (1MIU\_vs\_Placebo and 2MIU\_vs\_Placebo) were compared. A dose-  
45 dependent reaction was found for 260 out of 375 (69.3%) RefSeq common DEGs: increased  
46 transcripts showed a greater level of upregulation, and similarly, decreased DEGs were more  
47 downregulated following the higher dose administration of IL-2 (figure 1B). Consistently  
48 with this, the expression of four key Treg activation markers (*FOXP3*, *CTLA4*, *IKZF2*,  
49 *IL2RA*) showed a dose-proportional upregulation (figure 1C). Given the greater degree of  
50 immune-regulation promoted by 2MIU-IL-2, we focused on this higher-dose treatment for  
51 further analyses.  
52  
53  
54  
55  
56  
57  
58  
59  
60

## Gene expression changes during 2MIU-IL-2 treatment

Patients' transcriptomic differences between treatment and placebo groups throughout the administration period were assessed from the microarray data using Limma. Two comparisons,  $\Delta D8$  and  $\Delta D64$ , identified specific 2MIU-IL2-mediated changes at D8 and 64 compared to baseline and normalised to the placebo group.

The comparison  $\Delta D8$  identified 2635 RefSeq genes as significantly differentially expressed (1953 decreased, 682 increased), while only 525 RefSeq genes (198 decreased, 327 increased) resulted from  $\Delta D64$  (figure 2A, 2B). A widespread decrease in gene expression was reported after the first treatment cycle, while this effect seemed to be no longer present at later time points. In contrast, at D64 a more pronounced upregulation of gene expression was documented. Interestingly, in both comparisons, one of the most significant DEG is *FOXP3* which suggests an activation of Tregs starting from the first cycle and continuing throughout the administration period.

To understand the biological functions exerted by the identified DEGs, upregulated and downregulated lists of transcripts from the two comparisons were imported separately into Enrichr and GO analysis was conducted. The  $\Delta D8$  comparison revealed 448 downregulated GO BPs while  $\Delta D64$  showed only 35 downregulated significantly enriched terms. In contrast, analysis of upregulated DEGs identified 35 significantly enriched GO BPs in  $\Delta D64$  comparison while, only 10 processes were observed in  $\Delta D8$ .

The most significant  $\Delta D8$  GO BPs revealed alterations (both increase and decrease) in different processes involved in RNA metabolism at D8. These included variations in both non-coding RNA and mRNA processing, splicing and gene expression regulation (figure 3A and 3B). Moreover, evidence of inflammatory suppression was also documented, with neutrophil activation and degranulation being significantly decreased. In contrast, the top 10 significant GO BPs from  $\Delta D64$  did not show a clear inflammatory process downregulation, while inhibition of other mechanisms including iron transport and lipid processing were observed. However, several immune-regulatory processes, especially those involved in Treg-activation and differentiation were upregulated at D64. Interestingly, enrichment in muscle regulatory process was also documented (figure 3C and 3D).

## Pathway alteration during 2MIU-IL-2 treatment

The lists of significant DEGs ( $p\text{-value} < 0.05$  and  $1.2 \leq FC \leq -1.2$ ) outputted from  $\Delta D8$  and  $\Delta D64$  were imported into IPA to identify pathways altered longitudinally through the trial.

Seventy-seven pathways were altered in  $\Delta D8$ , the top twenty significant processes are displayed in figure 4A while the complete list is available in supplementary table 1. An inhibition of inflammatory mechanisms was identified, with functions of both innate (phagocytic cells, neutrophils, eosinophils, macrophages/monocytes and natural killers) and adaptive immune cells (cytotoxic T lymphocytes and B cells) being decreased. Moreover, inhibition of NF- $\kappa$ B and signalling related to several cytokines were documented.

Interestingly, negative regulation of pathways subserving autoimmune diseases, such as multiple sclerosis and systemic lupus erythematosus, were also found. Taken together, these results suggest a broader suppression of inflammatory processes, which are known to be activated in ALS, and also involved in other autoimmune pathologies. Additionally, the NRF2-mediated oxidative stress response pathway was decreased at D8 suggesting a reduction in oxidative stress. Moreover, two processes involved in CNS homeostasis, neuregulin and glioma signalling pathways, were inhibited.

Only 16 pathways were altered in  $\Delta D64$  (figure 4B and supplementary table 2). The majority of these were involved in the metabolism of several molecules including amino acids and sulphate-containing compounds. However, two mechanisms implicated in T-cell subset modulation were altered. In particular, activation of the Th2 pathway was observed.

Importantly, Th2 cells share some anti-inflammatory properties with Tregs mediated by IL-4 secretion<sup>18,19</sup>. These findings suggest an activation of immune-modulatory processes at the later trial stages. This is further confirmed by our data showing an increased expression of key mediators of Treg development, activation and functions following the last injection cycle compared to the first (figure 4C).

IPA diseases and functions' analysis revealed an almost opposite pathway regulation occurring at D8 and D64. In fact, while the vast majority of the pathways showed negative z-scores, which indicates inhibition, after the first cycle, a trend towards inversion was visible later on with a positive z-score-skewed phenotype (supplementary figure 2 and 3). This analysis reinforces previous observations indicating a rapid inhibition of inflammatory mechanisms after the first cycle. In fact, we have shown a repression of pathways involved in diapedesis of leukocytes -including phagocytes, monocytes, granulocytes and neutrophils- as well as developmental and functional inhibition of these cells. Cell death mechanisms were

1  
2  
3 also found to be activated in leukocytes (supplementary figure 2 and supplementary table 3).  
4 This may indicate a reorganization within immune cells happening at this time point.  
5 Concomitantly, downregulation of cell death processes in neurons and brain cells ("cell death  
6 of brain", " cell death of brain cells", "apoptosis of cortical neurons") was observed, together  
7 with a mild activation of the pro-survival "protection of cortical neurons" which is  
8 particularly interesting in the context of ALS (supplementary figure 2 and supplementary  
9 table 3). Furthermore, processes involved in metabolism, synthesis and production of reactive  
10 oxygen species (ROS) were inhibited at this time point.  
11 In contrast,  $\Delta D64$  analysis revealed an extensive activation of regulatory processes  
12 ("regulation of cells", "suppression of lymphocytes", "differentiation of induced Tregs",  
13 "regulation of mononuclear leukocytes" and "activation of Tregs") and concomitant  
14 activation of leukocyte apoptosis (supplementary figure 3). This suggested a more evident  
15 expansion of protective Tregs following the third cycle. However, unlike D8, processes  
16 involved in immune cell movement and recruitment seemed to increase at this time point.  
17 The reported activation of the "inflammatory response" process may be perceived as counter  
18 intuitive. However, when investigating the transcripts involved in this process by the  
19 software, it was clear that several anti-inflammatory agents (such as *FOXP3*, *IDO1*, *IL2RA*)  
20 were also included and thus "inflammatory response" included both pro and anti-  
21 inflammatory modulators (supplementary table 4).  
22  
23  
24  
25  
26  
27  
28  
29  
30  
31  
32  
33  
34  
35  
36  
37  
38

### 39 **Gene expression changes after 2MIU-IL-2 treatment**

40 Subsequently, we analysed the transcriptional changes which occurred in IMODALS patients  
41 during the follow-up period to investigate whether the 1d-IL-2 effect was sustained once  
42 treatment ceased. Limma was used to perform  $\Delta D85$  comparison. We found 508 RefSeq  
43 transcripts to be significantly differentially expressed (281 upregulated, 227 downregulated)  
44 (figure 5A). Interestingly, four main Treg activation markers -*FOXP3*, *IL2RA*, *CTLA4*,  
45 *IKZF2*- were no longer significantly differentially expressed. The comparison of their fold  
46 change from  $\Delta D85$  with the results retrieved from the previous analyses during drug  
47 administration - $\Delta D8$  and  $\Delta D64$ - showed that the expression of Treg markers progressively  
48 increased during the administration cycles, but it dramatically decreased once treatment  
49 ceased (figure 5B). This suggested that 2MIU-IL-2-promoted Treg activation was no longer  
50 preserved at D85. Furthermore, to investigate the biological functions of the upregulated and  
51 downregulated DEGs, a GO analysis was carried out. Twenty-five upregulated and 23  
52  
53  
54  
55  
56  
57  
58  
59  
60

1  
2  
3 downregulated significantly enriched GO BPs were found and none of these were related to  
4 immunological processes (supplementary figure 4A and B). Interestingly though, an  
5 upregulation in mechanisms involved in CNS development, including neural tube  
6 development and neuronal differentiation, were observed, while downregulation of  
7 neurotransmitter transport and axonogenesis was documented.  
8  
9  
10  
11  
12

### 13 **Microarray validation and variability in patient response**

14  
15 Microarray data validation was performed through qRT-PCR. Four key Treg markers  
16 (*FOXP3*, *IL2RA*, *CTLA4*, *IKZF2*) were chosen and samples from all 2MIU-IL-2-treated and  
17 placebo patients across all time points were screened. In line with microarray data, qRT-  
18 PCRs showed a time-dependent increase in the mRNA levels of these markers during the  
19 administration period which peaked at D64 (figure 6A). At D85 this upregulation was no  
20 longer sustained and transcripts showed levels more comparable to baseline. In contrast, no  
21 significant alterations were reported longitudinally within the placebo group. A considerable  
22 variability in the expression of Treg markers was registered amongst 2MIU-IL-2-treated  
23 patients. This suggested the existence of inter-individual variations in the response of ALS  
24 patients to the drug. This finding is in line with flow-cytometry data (figure 6B and  
25 previously published data <sup>32</sup>) showing a wide range of Treg count increases during the  
26 administration period (standard deviation of Treg cells measured at D8=101.7 and at  
27 D64=144.8). Given these results, we classified our 2MIU-IL-2-treated patients as low,  
28 moderate and high-Treg-responders according to their Treg levels registered at D64 (high =:  
29 Treg level at D64>250 cell/ul; moderate = Treg level between 250 and 150 cell/ul; low =  
30 Treg level at D64<150 cell/ul; see Table1). Importantly, no significant differences in age or  
31 in disease decline per month were reported amongst the three subgroups at baseline (One-  
32 way ANOVA with Tukey's correction).  
33  
34  
35  
36  
37  
38  
39  
40  
41  
42  
43  
44  
45  
46  
47

48 To further investigate these inter-individual dissimilarities and to evaluate the existence of  
49 key transcriptional patterns underlying the different magnitude of Treg expansion in low and  
50 high-Treg-responders, nanoString analyses were performed. In particular, we aimed to find  
51 immunological transcript dissimilarities in these participants across the administration period  
52 (D1, D8 and D64) and, for this reason, the nanoString autoimmune discovery panel was used.  
53 We performed a PCA analysis to visualise transcriptional-driven group separation (figure  
54 6C). High-Treg-responder samples from D8 and D64 appeared to be spatially distanced,  
55 whereas, placebo and low-Treg-responders were more dispersed and partially overlapped.  
56  
57  
58  
59  
60

1  
2  
3 Interestingly, low at D64 and high-Treg-responders at D1 were overlapping (figure 6C). We  
4 then identified a cluster of 81 discriminatory transcripts that were responsible for this PCA  
5 spatial separation (figure 6D). This included genes encoding both pro- and anti-inflammatory  
6 agents. At baseline, an almost opposite trend was reported between high and low-Treg-  
7 responders in this selected panel of transcripts.  
8  
9

10  
11 Lastly, pathway scoring analysis was performed. A sharp downregulation of pro-  
12 inflammatory pathways was reported in both high and low 2MIU-IL-2 Treg-responders  
13 (figure 7). However, baseline scores were considerably different between these two groups.  
14 Collectively, these results suggested that an almost opposite immunological phenotype  
15 characterized high and low-Treg-responders prior to drug administration. Therefore, this  
16 might have significantly influenced the participant reaction to 2MIU-IL-2.  
17  
18  
19  
20  
21  
22  
23

### 24 **Predictive biomarker identification**

25  
26 Given the inter-individual differences observed, we aimed to identify transcripts whose  
27 expression at D1 could predict 2MIU-IL-2-mediated Treg-response. In particular, we aimed  
28 to identify biomarkers of gene expression that could predict target engagement at the end of  
29 the trial (expressed as Tregs count at D64). To this end, we conducted a preliminary  
30 screening by correlating the expression of all the transcripts included in the autoimmune  
31 nanoString panel at D1 with Treg levels registered at D64 or with the expression of *IL2RA* at  
32 D64. Thirty-five genes showed expression levels at D1 which significantly correlated with  
33 both the variables and six biomarker candidates (*TLR9*, *SBNO2*, *CD27*, *BLNK*, *TRAF2*,  
34 *BTLA*) were selected which had the best correlation coefficients and statistical significance  
35 (supplementary table 5). However, given that only high and low-Treg-responders were  
36 screened through nanoString, the expression of these transcripts in all patients was  
37 investigated through qRT-PCR.  
38  
39

40  
41 *TLR9* and *CD27* were selected because their expression at D1 showed the best correlation  
42 with Treg count at D64. The rest of the proposed biomarkers instead did not significantly  
43 correlate and for this reason were excluded from further analyses (supplementary table 6). A  
44 strong negative correlation was observed for *TLR9* ( $R=-0.809$ ,  $R^2=0.654$ ,  $p$ -  
45 value=0.0014)(figure 8A). A milder positive correlation was reported for *CD27* ( $R=0.416$ ,  
46  $R^2=0.173$ ,  $p$ -value=0.179)(figure 8B).  
47  
48

49  
50 Expression data from *TLR9* and *CD27* at D1 were then combined and used as variables to  
51 create a more robust multiple linear regression model (figure 8C) which performed better  
52  
53  
54  
55  
56  
57  
58  
59  
60

1  
2  
3 than single linear models and with metrics which appeared encouraging ( $R^2=0.694$ ,  
4 Adjusted\_  $R^2=0.626$ ,  $p\text{-value}=0.005$ ). In particular, coefficient of determination ( $R^2$ ) and  
5 fitting root mean squared error (RMSE) obtained with this model were better than the values  
6 from *TLR9* alone ( $R^2_{\text{multiple}}=0.694$ ,  $\text{RMSE}_{\text{multiple}}=76.7$ ,  $R^2_{\text{TLR9}}=0.654$ ,  $\text{RMSE}_{\text{TLR9}}=81.4$ ).  
7  
8 Therefore, the computed multiple model formula (formula 1) could be used to predict ALS  
9 patient Treg count after three 2MIU-IL-2 administration cycles once the baseline level of  
10 *CD27* and *TLR9* expression is known.  
11  
12  
13  
14  
15  
16

17 **Formula 1:** *Treg number D64* =  $724.57 + (59.49 * CD27) + (-625.00 * TLR9)$   
18  
19

20 The model performance was assessed through leave-one-out cross-validation (LOOCV) and  
21 the emerging metric was computed ( $\text{RMSE}=84.28$ ). Although this might be perceived as a  
22 high score, it needs to be stressed that RMSE is a scale-dependent measurement which means  
23 that it needs to be interpreted in the context of the range of values assumed by the dependent  
24 variable (Treg count at D64). As mentioned before, the standard deviation for the Treg count  
25 was quite high ( $\text{SD}_{\text{Treg\_D64}}=144.8$ ) and thus, if compared with the LOOCV RMSE, we could  
26 conclude that the model was sufficiently robust when predicting new sets of data. Moreover,  
27 the predictive ability was also inspected correlating experimentally measured, or observed  
28 Treg counts at D64, with the predicted values (figure 8D). As expected, a strong positive  
29 correlation was observed ( $R=0.833$ ,  $p\text{-value}=0.0007$ ).  
30  
31  
32  
33  
34  
35  
36  
37  
38  
39  
40  
41  
42  
43  
44  
45  
46  
47  
48  
49  
50  
51  
52  
53  
54  
55  
56  
57  
58  
59  
60

## Discussion

Low-dose-IL-2 has been proposed as an immune-modulatory strategy for ALS to promote Treg expansion, dampen neuroinflammation and increase patient survival.<sup>39</sup> A pilot phase-II clinical trial was carried out to test the safety and activity of 1MIU or 2MIU-IL-2.<sup>32</sup> In the present report, transcriptomic profiling of patient leukocytes was performed to evaluate the effects of ld-IL-2 throughout the IMODALS trial.

Firstly, we assessed whether the two ld-IL-2 doses induced different reactions in IMODALS participants. To this end, microarray expression data at D64 from all treatment arms was compared. DEGs and GO enrichment analyses revealed an immune-regulation, with T-cell subset and the signaling related to several cytokines being altered in both treatment arms. This suggested that both doses efficiently promoted Treg expansion. However, 2MIU-IL-2 induced a more pronounced immune-regulation and a dose-dependent expression was identified for the majority (~70%) of the common DEGs. This is in line with results reported by Camu *et al.* which showed a dose-dependent increase in the percentage of Tregs.

Interestingly, ganglioside, ceramide and lipid metabolism were commonly altered at the end of both 1MIU and 2MIU-IL-2 treatment regimens. These mechanisms, especially ganglioside biosynthesis, have been implicated in the pathogenesis of ALS.<sup>40</sup> Thus, modulation of these metabolic processes could potentially contribute to the beneficial effects of ld-IL-2 on the pathophysiology of ALS. Given the dose-dependency, further analyses were conducted comparing only 2MIU-IL-2 with placebo participants.

We then analysed our microarray data longitudinally. A broad differential expression was observed in the comparison  $\Delta D8$ . This can be interpreted as a rapid response to the newly administered drug after the first treatment cycle. Over the trial course though, an adaptation probably occurred and less DEGs were reported in  $\Delta D64$ .

GO gene enrichment and IPA® analyses were carried out to identify pathways longitudinally altered throughout the trial. An inhibition of inflammatory processes was registered after the first administration cycle. In particular, transcripts associated with the function of both innate (neutrophils, eosinophils, macrophages and natural killers) and adaptive immune cells (cytotoxic T-cells and B-cells) were downregulated at D8. Of importance, evidence of dysregulation in these immune system cells is reported in the ALS literature. Neutrophil

1  
2  
3 activation correlates with disease severity and predicts patient survival. <sup>41-43</sup> Peripheral blood  
4 natural killer alterations and their infiltration into the spinal cord and motor cortex of ALS  
5 patients has been reported. <sup>44,45</sup> Although the role of monocytes/macrophages in ALS is still  
6 to be elucidated, recently, total CD14<sup>+</sup> monocyte levels appeared significantly higher, with  
7 increased M1 activation and pro-inflammatory features. <sup>17,46,47</sup> Moreover, adaptive immune  
8 system cells such as cytotoxic T-cells are known to infiltrate the CNS and to contribute to the  
9 loss of motor neurons. <sup>48,49</sup>

10  
11 NF- $\kappa$ B, cytokine signalling pathways and pathways promoting diapedesis of leukocytes were  
12 also down-regulated after the first cycle and these may contribute to the Id-IL-2-induced  
13 immune-suppression observed early after treatment initiation. Leukocyte cell death  
14 mechanisms were reported to be activated at this time point. However, this process specificity  
15 toward leukocytes should be investigated to exclude possible toxic effects on other cell types.  
16 Concomitantly, pathway analysis showed evidence of downregulation of cell death  
17 mechanisms in brain and cortical neurons which may indicate a positive pro-survival effect.  
18 Taken together these data suggest that the initial suppression of the immune system may have  
19 beneficial effects by dampening the widespread inflammation characteristic of ALS.

20  
21 This seems to be a short-term effect given that the downregulation of the majority of the  
22 inflammatory pathways was no longer present at D64. However, a robust activation of  
23 immune-regulatory processes was observed at this time point, with evidence of time-  
24 dependent activation of both Tregs and Th2 being observed. Of importance, Th2 share anti-  
25 inflammatory and neuroprotective properties with Tregs and both cell types are reduced in  
26 ALS patients <sup>18,19</sup>. Lymphocyte suppression and apoptosis induction was recorded at D64  
27 which might be due to the inhibitory action of Treg/Th2 cells on inflammatory mediators.  
28 Alongside immunological pathway alterations, Id-IL-2 appeared to affect other biological  
29 mechanisms. Metabolism, synthesis and production of ROS as well as the NRF2-mediated  
30 oxidative stress response pathways were inhibited at D8. Excessive ROS generation,  
31 oxidative stress and consequently oxidative damage are key mechanisms in the  
32 pathophysiology of ALS. <sup>50</sup> NRF2 is a transcription factor which promotes a cytoprotective  
33 response including induction of anti-oxidant and anti-inflammatory gene expression. <sup>51</sup>  
34  
35 Dysregulation in NRF2 signaling pathways has been reported in ALS and this is now  
36 considered a promising therapeutic target. <sup>52,53</sup> The observed NRF2 pathway inhibition may  
37 represent a detrimental short-term effect of Id-IL-2 given that this suppression was not  
38 detected at D64. However, considering the concurrent downregulation of mechanisms  
39 involved in ROS production, we can speculate that Id-IL-2 can instead have an anti-oxidant

1  
2  
3 effect by dampening the production of ROS and therefore reducing the need for the NRF2-  
4 associated stress response. However, further investigation is necessary to verify this  
5 hypothesis.  
6  
7  
8  
9

10 Subsequently, we investigated the transcriptional profiles of IMODALS participants during  
11 the post-treatment period. We found that the 1d-IL-2 immune-regulatory effect was no longer  
12 preserved at D85 and the expression of Treg markers was returning towards baseline levels.  
13 These findings are consistent with those reported by Camu *et al.* At the D85, GO enrichment  
14 analysis revealed no significant alteration in immunological processes. However, some CNS  
15 developmental mechanisms were upregulated (neural tube formation, development and  
16 closure and positive regulation of neuron differentiation) whereas processes involved in  
17 axonogenesis and neurotransmitter transport were downregulated.  
18  
19  
20  
21  
22  
23  
24  
25

26 Microarray validation was also carried out through qRT-PCR screening of four Treg markers.  
27 In line with the microarray data, a time-dependent increase in the expression of all of these  
28 transcripts was observed within the 2MIU-treated group whereas no significant changes were  
29 observed in placebo participants. In particular, the expression of Treg-specific markers  
30 peaked at D64, suggesting the existence of a cumulative reaction to successive doses of 1d-  
31 IL-2. In line with microarray data, at D85 these effects of 2MIU-IL-2 effect were no longer  
32 sustained. This analysis also revealed inter-individual differences in terms of the patient  
33 response to 1d-IL-2. This is consistent with data presented by Camu *et al* and the significant  
34 variability in terms of Treg expansion previously reported in clinical trials evaluating 1d-IL-2  
35 in several autoimmune disorders.<sup>26,28,54,55</sup>  
36  
37  
38  
39  
40  
41  
42  
43  
44

45 Thus, the aim was to investigate the existence of differences in participants' gene expression  
46 that could reflect the observed variation in Treg expansion. For this reason, patients were  
47 classified patients into high, moderate and low-Treg-responders depending on their Treg  
48 levels measured at D64. We then performed nanoString experiments to characterize  
49 immunological transcriptional differences between high and low-Treg-responding  
50 participants. We successfully identified an 81 transcript cluster which was able to  
51 discriminate between the two different groups. This analysis revealed an almost opposite  
52 immune phenotype at baseline between high and low-Treg-responders. Furthermore, pathway  
53 scoring analysis revealed that a considerable amount of inflammatory pathways were  
54 progressively downregulated in both types of 1d-IL-2 Treg-responders. However, a more  
55  
56  
57  
58  
59  
60

1  
2  
3 inflammatory-prone phenotype seemed to characterize low-Treg-responders at baseline. This  
4 might have exerted a significant influence on their ability to mount a strong Treg-response to  
5 ld-IL-2.  
6  
7

8  
9  
10 Finally, we aimed to identify smaller sets of transcripts capable of predicting the patient  
11 Treg-response to ld-IL-2. To this end, the expression of all the genes included in the  
12 nanoString panel at D1 was correlated with Treg levels<sup>32</sup> at D64. Two transcripts were  
13 selected: *TLR9* which showed a strong negative correlation and *CD27* which correlated  
14 positively with the D64 Treg count. Toll-like receptors (TLR) are a class of pattern  
15 recognition receptors implicated in pathogen identification and immune-response initiation.  
16 Dysregulation of TLR9 signaling has been associated with several autoimmune and  
17 neurodegenerative diseases.<sup>56,57</sup> Interestingly, increased *TLR9* expression was reported in the  
18 spinal cord of SOD1<sup>G93A</sup> transgenic mice.<sup>58</sup> *CD27* is a member of the tumor necrosis factor  
19 receptor family. The binding of its ligand, CD70, leads to immune cell activation and a pro-  
20 inflammatory response. However, CD27-CD70 has key role in Treg generation in the thymus  
21 and genetic ablation of either protein leads to a reduced number of thymic Tregs.<sup>59</sup>  
22 Moreover, CD27-deficiency caused reduction in Treg cell numbers.<sup>60,61</sup> Interestingly, Zhao  
23 *et al* reported *CD27* as one of the downregulated transcripts solely differentially expressed in  
24 the monocytes of rapidly progressive ALS patients.<sup>62</sup>  
25  
26 *TLR9* and *CD27* expression data was then combined and a robust multiple linear regression  
27 model with good predictive capacity ( $R^2= 0.694$ , Adjusted  $R^2= 0.626$ , p-value= 0.005) was  
28 generated. Therefore, the model formula should be able to forecast the magnitude of Treg  
29 expansion in ALS patients after measuring the baseline levels of *TLR9* and *CD27* expression.  
30 These can be considered as biomarkers of target engagement as their expression at  
31 recruitment is proposed to be predictive of cellular target stimulation and therefore Treg  
32 expansion promoted by three cycles of ld-IL-2. Importantly, if this pharmacological treatment  
33 provides evidence of clinical efficacy in ALS patients in future phase II/III trials, our model  
34 may be valuable for future precision medicine approaches, to allow patient stratification and  
35 identification of the best therapeutic strategy for each individual.  
36  
37  
38  
39  
40  
41  
42  
43  
44  
45  
46  
47  
48  
49  
50  
51  
52  
53

54  
55 A limitation of our study is the small participant group size, which particularly affects our  
56 analyses. In particular, we recognise age and sex as crucial variables possibly affecting ALS  
57 phenotype. However, in such a limited sized cohort, we believe that stratifying for these  
58 factors would have had a considerable impact in reducing the statistical power of our  
59  
60

1  
2  
3 analysis. Moreover, this limited participant size also substantially affected our proposed  
4 predictive biomarker research. However, preliminary evaluations are necessary to examine  
5 the safety and tolerability of new proposed drugs. Further investigation is needed to verify the  
6 immune-modulatory transcriptomic effect of ld-IL-2 and to validate our predictive model. To  
7 this end, a randomized, placebo-controlled, double-blind phase-II clinical trial, MIROCALS  
8 (NCT03039673), is currently active and aims to evaluate the effect of 2MIU-IL-2 in a larger  
9 ALS cohort of 220 participants. This will allow more complex examination of gene  
10 expression variations throughout the trial and further investigation of the variability in Treg-  
11 response as well as the validation of the robustness of our proposed predictive model.  
12  
13  
14  
15  
16  
17  
18  
19

20 In conclusion, transcriptional profiling of leukocytes from participants in the IMODALS trial  
21 revealed evidence of immune modulation following ld-IL-2 administration. Inter-individual  
22 differences in the treatment responses to 2MIU-IL-2 were observed and a two-biomarker-  
23 based model able to predict drug-induced Treg-response was identified. This could be  
24 particularly relevant in future precision medicine approaches for ALS.  
25  
26  
27  
28  
29

### 30 **Acknowledgments**

31 We are very grateful to ALS patients participating in the IMODALS trial who generously  
32 donated the biosamples underpinning this study.  
33  
34  
35  
36

### 37 **Funding information**

38 The IMODALS study was funded by a government call-for-tender for academic/investigator-  
39 driven research(French Ministry of Health, Programme Hospitalier de Recherche Clinique-  
40 Interrégional, 2014, n°14-056), the French ALS patient Association pour la recherche sur la  
41 Sclérose latérale amyotrophique and European Horizon2020 Grant no.633413.  
42  
43  
44  
45

46 IG and DW were funded by the National Institute for Health Research Sheffield Biomedical  
47 Research Centre for Translational Neuroscience (IS-BRC-1215-20017). The views expressed  
48 are those of the authors and not necessarily those of the NHS, the National Institute for  
49 Health Research or the Department of Health and Social Care. PJS is a National Institute for  
50 Health Research Senior Investigator (NF-SI-0617-10077). HZ is a Wallenberg Scholar.  
51  
52  
53

### 54 **Competing interests**

55 GB, TT, PNL, ML, CG, AM, PJS and JK have a patent relating to ld-IL-2 therapy for ALS  
56 (B75649EPD40021) pending.  
57  
58  
59  
60

## References

1. Hardiman O, Al-Chalabi A, Chio A, et al. Amyotrophic lateral sclerosis. *Nat Rev Dis Primers*. Oct 2017;3:17071. doi:10.1038/nrdp.2017.71
2. Nagoshi N, Nakashima H, Fehlings MG. Riluzole as a neuroprotective drug for spinal cord injury: from bench to bedside. *Molecules*. Apr 2015;20(5):7775-89. doi:10.3390/molecules20057775
3. Fang T, Al Khleifat A, Meurgey JH, et al. Stage at which riluzole treatment prolongs survival in patients with amyotrophic lateral sclerosis: a retrospective analysis of data from a dose-ranging study. *Lancet Neurol*. Mar 2018;doi:10.1016/S1474-4422(18)30054-1
4. GROUP WGOBOTEM-AS. Open-label 24-week extension study of edaravone (MCI-186) in amyotrophic lateral sclerosis. *Amyotroph Lateral Scler Frontotemporal Degener*. Oct 2017;18(sup1):55-63. doi:10.1080/21678421.2017.1364269
5. Edaravone Writing Group. Safety and efficacy of edaravone in well defined patients with amyotrophic lateral sclerosis: a randomised, double-blind, placebo-controlled trial. *Lancet Neurol*. Jul 2017;16(7):505-512. doi:10.1016/S1474-4422(17)30115-1
6. Writing group on behalf of the Edaravone (MCI-186) ALS 19 study group. Open-label 24-week extension study of edaravone (MCI-186) in amyotrophic lateral sclerosis. *Amyotroph Lateral Scler Frontotemporal Degener*. Oct 2017;18(sup1):55-63. doi:10.1080/21678421.2017.1364269
7. Mejzini R, Flynn LL, Pitout IL, Fletcher S, Wilton SD, Akkari PA. ALS Genetics, Mechanisms, and Therapeutics: Where Are We Now? *Front Neurosci*. 2019;13:1310. doi:10.3389/fnins.2019.01310
8. Taylor JP, Brown RH, Cleveland DW. Decoding ALS: from genes to mechanism. *Nature*. 11 2016;539(7628):197-206. doi:10.1038/nature20413
9. Ferraiuolo L, Kirby J, Grierson AJ, Sendtner M, Shaw PJ. Molecular pathways of motor neuron injury in amyotrophic lateral sclerosis. *Nat Rev Neurol*. Nov 2011;7(11):616-30. doi:10.1038/nrneurol.2011.152
10. Liu J, Wang F. Role of Neuroinflammation in Amyotrophic Lateral Sclerosis: Cellular Mechanisms and Therapeutic Implications. *Front Immunol*. 2017;8:1005. doi:10.3389/fimmu.2017.01005
11. Sharma A, Rudra D. Emerging Functions of Regulatory T Cells in Tissue Homeostasis. *Front Immunol*. 2018;9:883. doi:10.3389/fimmu.2018.00883
12. Mantovani S, Garbelli S, Pasini A, et al. Immune system alterations in sporadic amyotrophic lateral sclerosis patients suggest an ongoing neuroinflammatory process. *J Neuroimmunol*. May 2009;210(1-2):73-9. doi:10.1016/j.jneuroim.2009.02.012
13. Rentzos M, Evangelopoulos E, Sereti E, et al. Alterations of T cell subsets in ALS: a systemic immune activation? *Acta Neurol Scand*. Apr 2012;125(4):260-4. doi:10.1111/j.1600-0404.2011.01528.x
14. Beers DR, Zhao W, Wang J, et al. ALS patients' regulatory T lymphocytes are dysfunctional, and correlate with disease progression rate and severity. *JCI Insight*. Mar 2017;2(5):e89530. doi:10.1172/jci.insight.89530
15. Henkel JS, Beers DR, Wen S, et al. Regulatory T-lymphocytes mediate amyotrophic lateral sclerosis progression and survival. *EMBO Mol Med*. 01 2013;5(1):64-79. doi:10.1002/emmm.201201544

16. Sheean RK, McKay FC, Cretney E, et al. Association of Regulatory T-Cell Expansion With Progression of Amyotrophic Lateral Sclerosis: A Study of Humans and a Transgenic Mouse Model. *JAMA Neurol.* Mar 2018;doi:10.1001/jamaneurol.2018.0035
17. Jin M, Günther R, Akgün K, Hermann A, Ziemssen T. Peripheral proinflammatory Th1/Th17 immune cell shift is linked to disease severity in amyotrophic lateral sclerosis. *Sci Rep.* Apr 2020;10(1):5941. doi:10.1038/s41598-020-62756-8
18. Beers DR, Henkel JS, Zhao W, et al. Endogenous regulatory T lymphocytes ameliorate amyotrophic lateral sclerosis in mice and correlate with disease progression in patients with amyotrophic lateral sclerosis. *Brain.* May 2011;134(Pt 5):1293-314. doi:10.1093/brain/awr074
19. Zhao W, Beers DR, Liao B, Henkel JS, Appel SH. Regulatory T lymphocytes from ALS mice suppress microglia and effector T lymphocytes through different cytokine-mediated mechanisms. *Neurobiol Dis.* Dec 2012;48(3):418-28. doi:10.1016/j.nbd.2012.07.008
20. Zhao W, Beers DR, Appel SH. Immune-mediated mechanisms in the pathoprosession of amyotrophic lateral sclerosis. *J Neuroimmune Pharmacol.* Sep 2013;8(4):888-99. doi:10.1007/s11481-013-9489-x
21. Alsuliman A, Appel SH, Beers DR, et al. A robust, good manufacturing practice-compliant, clinical-scale procedure to generate regulatory T cells from patients with amyotrophic lateral sclerosis for adoptive cell therapy. *Cytotherapy.* 10 2016;18(10):1312-24. doi:10.1016/j.jcyt.2016.06.012
22. Cheng G, Yu A, Malek TR. T-cell tolerance and the multi-functional role of IL-2R signaling in T-regulatory cells. *Immunol Rev.* May 2011;241(1):63-76. doi:10.1111/j.1600-065X.2011.01004.x
23. Toomer KH, Lui JB, Altman NH, Ban Y, Chen X, Malek TR. Essential and non-overlapping IL-2R $\alpha$ -dependent processes for thymic development and peripheral homeostasis of regulatory T cells. *Nat Commun.* 03 2019;10(1):1037. doi:10.1038/s41467-019-08960-1
24. Ito S, Bollard CM, Carlsten M, et al. Ultra-low dose interleukin-2 promotes immune-modulating function of regulatory T cells and natural killer cells in healthy volunteers. *Mol Ther.* Jul 2014;22(7):1388-1395. doi:10.1038/mt.2014.50
25. Saadoun D, Rosenzweig M, Joly F, et al. Regulatory T-cell responses to low-dose interleukin-2 in HCV-induced vasculitis. *N Engl J Med.* Dec 2011;365(22):2067-77. doi:10.1056/NEJMoa1105143
26. Hartemann A, Bensimon G, Payan CA, et al. Low-dose interleukin 2 in patients with type 1 diabetes: a phase 1/2 randomised, double-blind, placebo-controlled trial. *Lancet Diabetes Endocrinol.* Dec 2013;1(4):295-305. doi:10.1016/S2213-8587(13)70113-X
27. Rosenzweig M, Churlaud G, Mallone R, et al. Low-dose interleukin-2 fosters a dose-dependent regulatory T cell tuned milieu in T1D patients. *J Autoimmun.* Apr 2015;58:48-58. doi:10.1016/j.jaut.2015.01.001
28. Castela E, Le Duff F, Butori C, et al. Effects of low-dose recombinant interleukin 2 to promote T-regulatory cells in alopecia areata. *JAMA Dermatol.* Jul 2014;150(7):748-51. doi:10.1001/jamadermatol.2014.504
29. Humrich JY, Riemekasten G. Low-dose interleukin-2 therapy for the treatment of systemic lupus erythematosus. *Curr Opin Rheumatol.* 03 2019;31(2):208-212. doi:10.1097/BOR.0000000000000575
30. Kennedy-Nasser AA, Ku S, Castillo-Caro P, et al. Ultra low-dose IL-2 for GVHD prophylaxis after allogeneic hematopoietic stem cell transplantation mediates expansion of

- regulatory T cells without diminishing antiviral and antileukemic activity. *Clin Cancer Res.* Apr 2014;20(8):2215-25. doi:10.1158/1078-0432.CCR-13-3205
31. He J, Zhang R, Shao M, et al. Efficacy and safety of low-dose IL-2 in the treatment of systemic lupus erythematosus: a randomised, double-blind, placebo-controlled trial. *Ann Rheum Dis.* 01 2020;79(1):141-149. doi:10.1136/annrheumdis-2019-215396
32. Camu W, Mickunas M, Veyrone JL, et al. Repeated 5-day cycles of low dose aldesleukin in amyotrophic lateral sclerosis (IMODALS): A phase 2a randomised, double-blind, placebo-controlled trial. *EBioMedicine.* Jul 2020:102844. doi:10.1016/j.ebiom.2020.102844
33. Ritchie ME, Phipson B, Wu D, et al. limma powers differential expression analyses for RNA-sequencing and microarray studies. *Nucleic Acids Res.* Apr 2015;43(7):e47. doi:10.1093/nar/gkv007
34. Nygaard V, Rødland EA, Hovig E. Methods that remove batch effects while retaining group differences may lead to exaggerated confidence in downstream analyses. *Biostatistics.* Jan 2016;17(1):29-39. doi:10.1093/biostatistics/kxv027
35. Chen EY, Tan CM, Kou Y, et al. Enrichr: interactive and collaborative HTML5 gene list enrichment analysis tool. *BMC Bioinformatics.* Apr 2013;14:128. doi:10.1186/1471-2105-14-128
36. Kuleshov MV, Jones MR, Rouillard AD, et al. Enrichr: a comprehensive gene set enrichment analysis web server 2016 update. *Nucleic Acids Res.* 07 2016;44(W1):W90-7. doi:10.1093/nar/gkw377
37. Supek F, Bošnjak M, Škunca N, Šmuc T. REVIGO summarizes and visualizes long lists of gene ontology terms. *PLoS One.* 2011;6(7):e21800. doi:10.1371/journal.pone.0021800
38. Krämer A, Green J, Pollard J, Tugendreich S. Causal analysis approaches in Ingenuity Pathway Analysis. *Bioinformatics.* Feb 2014;30(4):523-30. doi:10.1093/bioinformatics/btt703
39. Giovannelli I, Heath P, Shaw PJ, Kirby J. The involvement of regulatory T cells in amyotrophic lateral sclerosis and their therapeutic potential. *Amyotroph Lateral Scler Frontotemporal Degener.* Jun 2020:1-10. doi:10.1080/21678421.2020.1752246
40. Moll T, Shaw PJ, Cooper-Knock J. Disrupted glycosylation of lipids and proteins is a cause of neurodegeneration. *Brain.* May 2020;143(5):1332-1340. doi:10.1093/brain/awz358
41. Choi SJ, Hong YH, Kim SM, Shin JY, Suh YJ, Sung JJ. High neutrophil-to-lymphocyte ratio predicts short survival duration in amyotrophic lateral sclerosis. *Sci Rep.* 01 2020;10(1):428. doi:10.1038/s41598-019-57366-y
42. Swindell WR, Kruse CPS, List EO, Berryman DE, Kopchick JJ. ALS blood expression profiling identifies new biomarkers, patient subgroups, and evidence for neutrophilia and hypoxia. *J Transl Med.* 05 2019;17(1):170. doi:10.1186/s12967-019-1909-0
43. McGill RB. Monocytes and neutrophils are associated with clinical features in amyotrophic lateral sclerosis. In: Frederik J Steyn STN, Kathryn A Thorpe, Susan Heggie, Marc J Ruitenberg, Robert D Henderson, Pamela A McCombe, Trent M Woodruff, editor.: *Brain Communications*; 2020.
44. Gustafson MP, Staff NP, Bornschlegl S, et al. Comprehensive immune profiling reveals substantial immune system alterations in a subset of patients with amyotrophic lateral sclerosis. *PLoS One.* 2017;12(7):e0182002. doi:10.1371/journal.pone.0182002
45. Garofalo S, Coccozza G, Porzia A, et al. Natural killer cells modulate motor neuron-immune cell cross talk in models of Amyotrophic Lateral Sclerosis. *Nat Commun.* Apr 2020;11(1):1773. doi:10.1038/s41467-020-15644-8

- 1
- 2
- 3
- 4 46. McCombe PA, Lee JD, Woodruff TM, Henderson RD. The Peripheral Immune System
- 5 and Amyotrophic Lateral Sclerosis. *Front Neurol.* 2020;11:279.
- 6 doi:10.3389/fneur.2020.00279
- 7 47. Du Y, Zhao W, Thonhoff JR, Wang J, Wen S, Appel SH. Increased activation ability of
- 8 monocytes from ALS patients. *Exp Neurol.* Jun 2020;328:113259.
- 9 doi:10.1016/j.expneurol.2020.113259
- 10 48. Coque E, Salsac C, Espinosa-Carrasco G, et al. Cytotoxic CD8. *Proc Natl Acad Sci U S A.*
- 11 02 2019;116(6):2312-2317. doi:10.1073/pnas.1815961116
- 12 49. Nardo G, Trolese MC, Verderio M, et al. Counteracting roles of MHCI and CD8. *Mol*
- 13 *Neurodegener.* 08 2018;13(1):42. doi:10.1186/s13024-018-0271-7
- 14 50. Barber SC, Shaw PJ. Oxidative stress in ALS: key role in motor neuron injury and
- 15 therapeutic target. *Free Radic Biol Med.* Mar 2010;48(5):629-41.
- 16 doi:10.1016/j.freeradbiomed.2009.11.018
- 17 51. Sivandzade F, Prasad S, Bhalariao A, Cucullo L. NRF2 and NF- $\kappa$ B interplay in
- 18 cerebrovascular and neurodegenerative disorders: Molecular mechanisms and possible
- 19 therapeutic approaches. *Redox Biol.* 02 2019;21:101059. doi:10.1016/j.redox.2018.11.017
- 20 52. Johnson DA, Johnson JA. Nrf2--a therapeutic target for the treatment of
- 21 neurodegenerative diseases. *Free Radic Biol Med.* Nov 2015;88(Pt B):253-267.
- 22 doi:10.1016/j.freeradbiomed.2015.07.147
- 23 53. Mead RJ, Higginbottom A, Allen SP, et al. S[+] Apomorphine is a CNS penetrating
- 24 activator of the Nrf2-ARE pathway with activity in mouse and patient fibroblast models of
- 25 amyotrophic lateral sclerosis. *Free Radic Biol Med.* Aug 2013;61:438-52.
- 26 doi:10.1016/j.freeradbiomed.2013.04.018
- 27 54. Koreth J, Matsuoka K, Kim HT, et al. Interleukin-2 and regulatory T cells in graft-
- 28 versus-host disease. *N Engl J Med.* Dec 2011;365(22):2055-66. doi:10.1056/NEJMoa1108188
- 29 55. He J, Zhang R, Shao M, et al. Efficacy and safety of low-dose IL-2 in the treatment of
- 30 systemic lupus erythematosus: a randomised, double-blind, placebo-controlled trial. *Ann*
- 31 *Rheum Dis.* 01 2020;79(1):141-149. doi:10.1136/annrheumdis-2019-215396
- 32 56. Fiebich BL, Batista CRA, Saliba SW, Yousif NM, de Oliveira ACP. Role of Microglia TLRs
- 33 in Neurodegeneration. *Front Cell Neurosci.* 2018;12:329. doi:10.3389/fncel.2018.00329
- 34 57. Marongiu L, Gornati L, Artuso I, Zanoni I, Granucci F. Below the surface: The inner
- 35 lives of TLR4 and TLR9. *J Leukoc Biol.* 07 2019;106(1):147-160. doi:10.1002/JLB.3MIR1218-
- 36 483RR
- 37 58. Letiembre M, Liu Y, Walter S, et al. Screening of innate immune receptors in
- 38 neurodegenerative diseases: a similar pattern. *Neurobiol Aging.* May 2009;30(5):759-68.
- 39 doi:10.1016/j.neurobiolaging.2007.08.018
- 40 59. Coquet JM, Ribot JC, Bąbała N, et al. Epithelial and dendritic cells in the thymic
- 41 medulla promote CD4+Foxp3+ regulatory T cell development via the CD27-CD70 pathway. *J*
- 42 *Exp Med.* Apr 2013;210(4):715-28. doi:10.1084/jem.20112061
- 43 60. Winkels H, Meiler S, Lievens D, et al. CD27 co-stimulation increases the abundance of
- 44 regulatory T cells and reduces atherosclerosis in hyperlipidaemic mice. *Eur Heart J.* 12
- 45 2017;38(48):3590-3599. doi:10.1093/eurheartj/ehx517
- 46 61. Claus C, Riether C, Schürch C, Matter MS, Hilmenyuk T, Ochsenbein AF. CD27
- 47 signaling increases the frequency of regulatory T cells and promotes tumor growth. *Cancer*
- 48 *Res.* Jul 2012;72(14):3664-76. doi:10.1158/0008-5472.CAN-11-2791
- 49
- 50
- 51
- 52
- 53
- 54
- 55
- 56
- 57
- 58
- 59
- 60

1  
2  
3 62. Zhao W, Beers DR, Hooten KG, et al. Characterization of Gene Expression Phenotype  
4 in Amyotrophic Lateral Sclerosis Monocytes. *JAMA Neurol.* Jun 2017;74(6):677-685.  
5 doi:10.1001/jamaneurol.2017.0357  
6  
7  
8  
9  
10  
11  
12  
13  
14  
15  
16  
17  
18  
19  
20  
21  
22  
23  
24  
25  
26  
27  
28  
29  
30  
31  
32  
33  
34  
35  
36  
37  
38  
39  
40  
41  
42  
43  
44  
45  
46  
47  
48  
49  
50  
51  
52  
53  
54  
55  
56  
57  
58  
59  
60

## Figure Legends

**Figure 1. End of the treatment (D64) analysis and dose-dependency.** (A) Venn diagram showing significant ( $p$ -value  $< 0.05$ ) differentially expressed genes (DEGs) from either 1MIU\_vs\_Placebo or 2MIU\_vs\_Placebo TAC (Transcriptome analysis console) comparisons. All altered transcripts are reported in brackets while RefSeq annotated transcripts are shown in bold. Overlapping common DEGs are also shown. For each RefSeq transcript list shown in the Venn diagram, the top 10 significant enriched Gene Ontology (GO) biological processes are plotted. X axis:  $-\log_{10}$  (enrichment  $p$ -value); y axis: GO term. (B) Scatter plot displaying 375 RefSeq DEGs altered in common within the two treatment groups and their fold changes resulting from either 1MIU\_vs\_Placebo (X-axis) or 2MIU\_vs\_Placebo (Y-axis) comparisons. 260 out of 375 genes (69.3%) show a dose-dependent expression (in blue) while transcripts showing no dose-dependent trend are represented in red. (C) The expression levels (SST-RMA normalised  $\log_2$  of signal intensity from the microarrays) of 4 Treg activation markers – *FOXP3*, *CTLA4*, *IKZF2* and *IL2RA* – are shown. A significant dose-dependent upregulation of these transcripts is detected. Box plots show mean  $\pm$  SD. A two-way ANOVA with Tukey's correction for multiple comparisons was conducted. \*: Adjusted  $p$ -value  $< 0.05$ , \*\*: Adjusted  $p$ -value  $< 0.01$ , \*\*\*: Adjusted  $p$ -value  $< 0.001$ , \*\*\*\*: Adjusted  $p$ -value  $< 0.0001$ . SST-RMA= signal space transformation robust multi-chip analysis method for microarray data normalization.

**Figure 2. Transcriptional changes during 2MIU-IL2 administration.** Volcano plots displaying differentially expressed genes (DEGs) resulting from the comparisons  $\Delta D8$  (A) and  $\Delta D64$  (B). DEGs are plotted and colour-coded depending on their fold change (FC) and their significance levels ( $-\log_{10}$   $p$ -value): non-significant or transcripts that failed the FC cut-off are reported in grey, significant and with  $FC \leq -1.2$  in blue and significant and with  $FC \geq 1.2$  in red. Three black lines are also shown: the horizontal line indicates the significance threshold ( $-\log_{10}$   $p$ -value = 1.3) and two vertical dotted lines mark the FC cut-off at -1.2 and 1.2 respectively. A widespread downregulation is detectable at D8, while at D64 an increased upregulation is reported amongst which some Treg makers are recognisable. (Empirical Bayesian statistics was conducted using Limma to find significant DEGs).

**Figure 3. Altered biological processes during 2MIU-IL2 administration.** Bar plots resulting from GO Biological Processes (GO BP) enrichment analysis. In particular, the top 10 significant downregulated (A) and upregulated (B) GO BPs from  $\Delta D8$  and top 10 significant downregulated (C) and upregulated (D) GO BPs from  $\Delta D64$  are shown. Significance threshold lines are reported in black ( $-\log_{10}$   $p$ -value = 1.3). A significant downregulation of pro-inflammatory processes involving neutrophils and an alteration in the RNA metabolism are observed at D8 while, later during the course of the trial, a significant upregulation of Treg processes is documented. (Fisher's exact statistical test was performed using Enrichr to cluster transcripts into GO BP terms).

**Figure 4. Ingenuity Pathway Analysis (IPA).** Bar plots displaying top 20 significant IPA canonical pathways. Activated ( $z$ -score  $> 0$ , in orange) or inhibited pathways ( $z$ -score  $< 0$ , in blue) resulting from the analysis  $\Delta D8$  (A) and  $\Delta D64$  (B) are shown. Significant pathways but with  $z$ -score equal to 0 (in white) or with no activation prediction available in the software (in grey) are also reported. A significance threshold line is displayed in orange ( $-\log_{10}$   $p$ -value = 1.3). A widespread downregulation of inflammatory pathways is detectable at D8 while fewer pathways are altered at D64. However, activation of Th2 is reported. (A right-tailed Fisher's Exact test was conducted to calculate significantly altered pathways and the  $z$ -score was computed to predict the activation state of each mechanism). (C) Customized

pathways created with IPA displaying key regulators of activation, development and functions of Tregs. In particular, two pathway maps displaying fold changes (FCs) from  $\Delta D8$  and  $\Delta D64$  are juxtaposed for comparison. Significant ( $p$ -value $<0.05$ ) differentially expressed genes are shown in bold and their gene symbol is underlined. A more prominent upregulation of Treg genes is reported at D64. Data were analyzed through the use of IPA (QIAGEN Inc., <https://www.qiagenbioinformatics.com/products/ingenuitypathway-analysis>).

**Figure 5. Transcriptional changes during the follow-up period.** (A) Volcano plot showing differentially expressed genes (DEGs) resulting from the comparisons  $\Delta D85$ . DEGs are plotted and colour-coded depending on their fold change (FC) and their significance levels ( $-\text{Log}_{10}$   $p$ -value): non-significant transcripts or transcripts that failed the FC cut-off are reported in grey, significant and with  $\text{FC} \leq -1.2$  in blue and significant and with  $\text{FC} \geq 1.2$  in red. Three black lines are also shown: the horizontal line indicates the significance threshold ( $-\text{Log}_{10}$   $p$ -value=1.3 or  $p$ -value=0.05) and the two vertical dotted lines mark the FC cut-offs at -1.2 and 1.2 respectively. (Empirical Bayesian statistics was conducted using Limma to find significant DEGs). (B) Plot displaying the variation in the expression of four key Treg activation markers – *FOXP3*, *IL2RA*, *CTLA4* and *IKZF2* – throughout and after the administration period. Their expression increases during the 2MIU-IL-2 treatment and peaks at D64 but the levels of expression decrease at D85. On the x-axis the different Limma comparisons are shown while on the y-axis the FC for each transcript is reported.

**Figure 6. Microarray validation and patient variability.**

(A) Graphs showing expression of *FOXP3*, *IL2RA*, *CTLA4* and *IKZF2* in 2MIU-IL-2 treated (in red) and placebo (in blue) patients at the four different time points (D1, D8, D64 and D85). Data were generated through qRT-PCR. A time-dependent activation of these markers is reported in the 2MIU-IL-2 group. Box plots display mean  $\pm$  SD (technical replicates=3). A two-way ANOVA with either Sidak (for comparisons between different treatment regimens, significant differences indicated with \*) or Tukey (for comparisons between time points within the same treatment type, significant differences indicated with #) correction for multiple comparisons was conducted. \* or #: Adjusted  $p$ -value $<0.05$ , \*\* or ###: Adjusted  $p$ -value $<0.01$ . (B) Graph displaying the number of Tregs per  $\mu\text{l}$  of blood of each 2MIU IL-2-treated participant at each time point (Flow-cytometry data). Patients are shown with different colours and their IDs are reported in the legend (C) PCA plot summarising expression differences between samples depending on treatment regimen and time point (colour code legend is reported. H 2MIU D1, D8, D64= high-Treg-responders at D1, D8 and D64; L 2MIU D1, D8, D64= low-Treg-responders at D1, D8 and D64 and Placebo at D1, D8 and D64). High-Treg-responders from D8 and D64 are the most different samples. (Quocore multi group comparison statistical test,  $p$ -value $<0.05$ ) (D) Hierarchically clustered heatmap displaying differences in the expression of 81 transcripts identified as discriminating variables from the PCA analysis in fig 6B. Gene expression variations across sample groups (H 2MIU D1, D8, D64= high-Treg-responders at D1, D8 and D64; L 2MIU D1, D8, D64= low-Treg-responders at D1, D8 and D64 and Placebo at D1, D8 and D64) are displayed as z-scores (positive z-scores in red, negative in blue). An opposite expression between high and low-Treg-responders is detectable, especially at D1.

**Figure 7. Pathway scoring analysis.** Graph showing results from the pathway scoring analysis performed using Advanced Analysis nSolver software. Pathway activation scores are plotted as a function of the different treatment type and time points (H 2MIU D1, D8, D64= high-Treg-responders at D1, D8 and D64; L 2MIU D1, D8, D64= low-Treg-responders at D1, D8 and D64 and Placebo at D1, D8 and D64). An evident downregulation of several

1  
2  
3 inflammatory pathways is demonstrated in both high and low-Treg-responders although  
4 baseline differences were observed between the two treated subgroups.  
5  
6

7 **Figure 8. Biomarker identification analysis.** Linear regression models describing the  
8 correlation between the expression of *TLR9* (A) and *CD27* (B) at the baseline (D1) and the  
9 Treg number at D64 for each 2MIU-IL-2 treated patient. Each dot represents a trial  
10 participant (average expression values computed from 3 qRT-PCR experiments, N=3) and  
11 they are colour-coded depending on their Treg-response type: high (orange dots), moderate  
12 (yellow squares) and low (green triangles). A regression line (black) and its regression  
13 confidence bands (grey) are also shown. Linear regression model for *TLR9* (A:  $R = -0.809$ ,  
14  $R^2 = 0.654$ ,  $p\text{-value} = 0.0014$ ) was stronger than the model for *CD27* (B:  $R = 0.416$ ,  $R^2 = 0.173$ ,  
15  $p\text{-value} = 0.179$ ) (C) Multiple linear regression analysis indicating the relationship between 2  
16 predictors (expression of *TLR9* and *CD27* at D1) and the response variable (number of Tregs  
17 at D64). A good prediction model was obtained ( $R^2 = 0.6937$  and  $p\text{-value} = 0.00487$ ). Each dot  
18 represents a patient and they are colour-coded depending on their Treg-response type: high  
19 (orange dots), moderate (yellow squares) and low (green triangles). The regression plane is  
20 also displayed in black. (D) Plot showing the correlation between flow-cytometry-measured  
21 Treg counts (observed, X-axis) and Treg numbers predicted by our multiple linear model  
22 (predicted, Y-axis). Correlation metrics ( $R = 0.833$ ,  $R^2 = 0.693$ ,  $p\text{-value} = 0.0007$ ) suggest an  
23 acceptable predictive model. Each dot represents a sample and a red dotted regression line is  
24 also shown.  
25  
26  
27  
28  
29  
30  
31  
32  
33  
34  
35  
36  
37  
38  
39  
40  
41  
42  
43  
44  
45  
46  
47  
48  
49  
50  
51  
52  
53  
54  
55  
56  
57  
58  
59  
60

Patient ID	Gender	Treatment type	Age at D1	Disease decline per month	Treg count at D64	2MIU-treated response classification
C01P001	Male	1MIU-IL-2	40.2	0.114	115.14	-
C01P005	Male	1MIU-IL-2	42.5	0.514	145.97	-
C01P008	Female	1MIU-IL-2	47.7	0.400	120.59	-
C01P010	Female	1MIU-IL-2	65.4	0.378	151.50	-
C01P013	Male	1MIU-IL-2	44.7	0.643	114.18	-
C01P020	Female	1MIU-IL-2	46.4	0.296	160.49	-
C01P023	Male	1MIU-IL-2	53.8	0.075	87.79	-
C01P024	Female	1MIU-IL-2	55.8	0.600	156.26	-
C01P027	Male	1MIU-IL-2	64.4	0.800	154.40	-
C01P033	Male	1MIU-IL-2	59.1	0.250	91.62	-
C01P035	Female	1MIU-IL-2	75.4	0.424	146.48	-
C01P038	Male	1MIU-IL-2	64.4	0.224	81.65	-
C01P003	Male	2MIU-IL-2	36.5	1.000	406.72	High
C01P004	Female	2MIU-IL-2	47.3	0.688	169.13	Moderate
C01P009	Female	2MIU-IL-2	68.8	0.692	434.47	High
C01P011	Male	2MIU-IL-2	76.6	1.500	144.34	Low
C01P016	Male	2MIU-IL-2	63.4	0.375	88.99	Low
C01P018	Male	2MIU-IL-2	59.8	0.444	117.88	Low
C01P021	Female	2MIU-IL-2	62.7	0.226	505.70	High
C01P026	Male	2MIU-IL-2	72.5	0.417	222.66	Moderate
C01P028	Male	2MIU-IL-2	63.4	0.148	176.08	Moderate
C01P032	Male	2MIU-IL-2	44.4	0.667	181.13	Moderate
C01P036	Male	2MIU-IL-2	56.5	0.209	52.22	Low
C01P037	Male	2MIU-IL-2	40.3	1.375	263.93	High
C01P002	Male	Placebo	47.5	0.375	30.08	-
C01P006	Male	Placebo	44.2	0.277	34.22	-
C01P007	Male	Placebo	49.2	0.351	55.14	-
C01P012	Female	Placebo	64.6	0.455	35.41	-
C01P014	Male	Placebo	52.6	0.350	90.37	-
C01P017	Male	Placebo	42.2	0.143	60.33	-
C01P022	Male	Placebo	63.6	0.429	32.99	-
C01P025	Male	Placebo	61.7	0.909	84.88	-
C01P030	Male	Placebo	58.5	0.313	25.63	-
C01P031	Male	Placebo	53.9	1.600	46.73	-
C01P034	Female	Placebo	69.7	0.579	57.52	-
C01P039	Female	Placebo	69.7	0.241	32.49	-

**Table 1: Patient characteristics and response type.**

This table illustrates the gender, age, disease decline per month and treatment regimen of each participant. Moreover, Treg count at D64 is displayed and these data have been used to classify the patient response to 2MIU-IL-2 (high responders: Treg level at D64 > 250 cells/ul; moderate responders: between 150 and 250 cells/ul; low responders: < 150 cells/ul).

# Figure 1

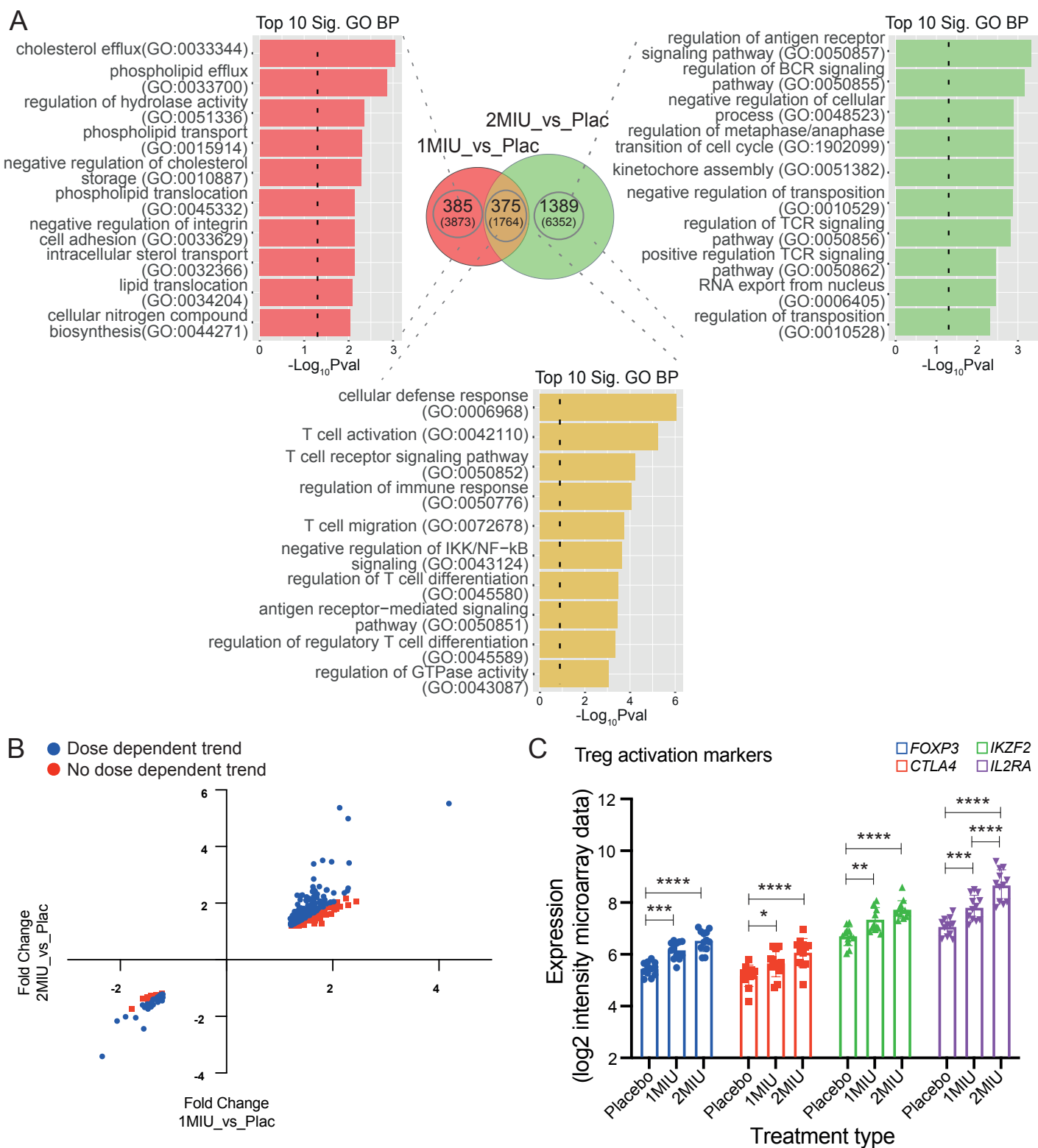
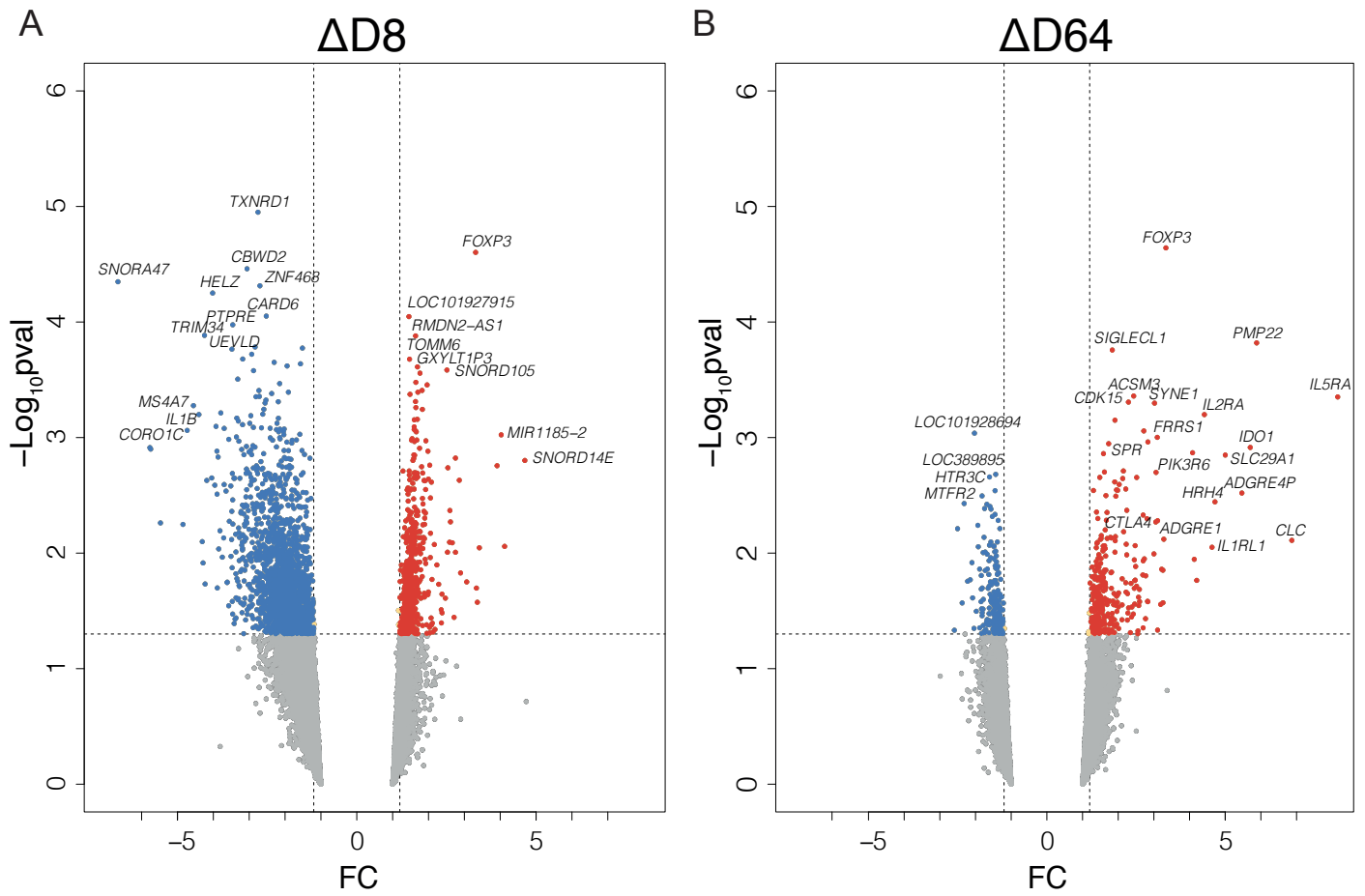


# Figure 2

Legend ■ NS ■ Downregulated ■ Upregulated



Downloaded from https://academic.oup.com/braincomms/advance-article/doi/10.1093/braincomms/fcab141/6311265 by guest on 06 July 2021

# Figure 3

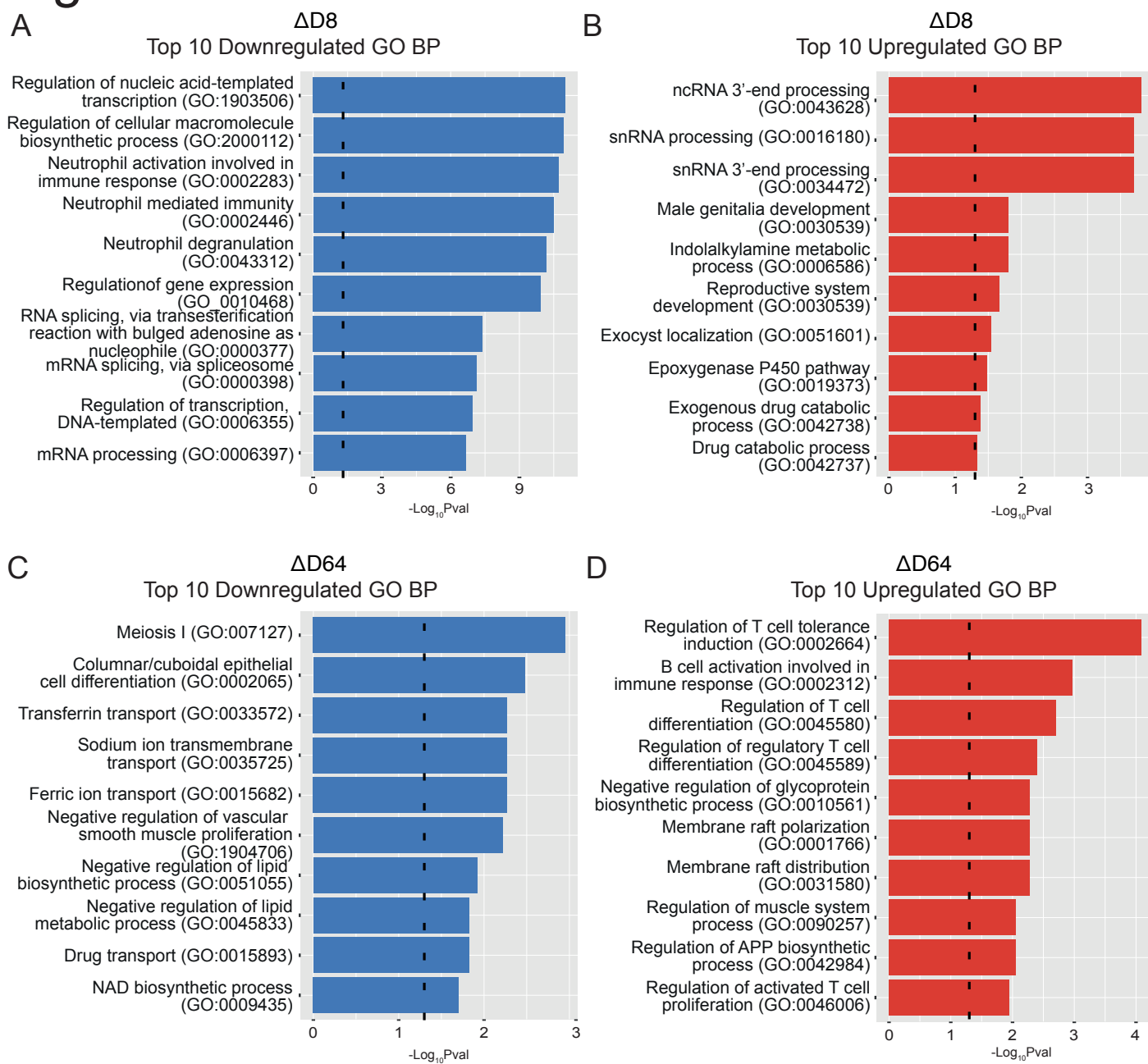
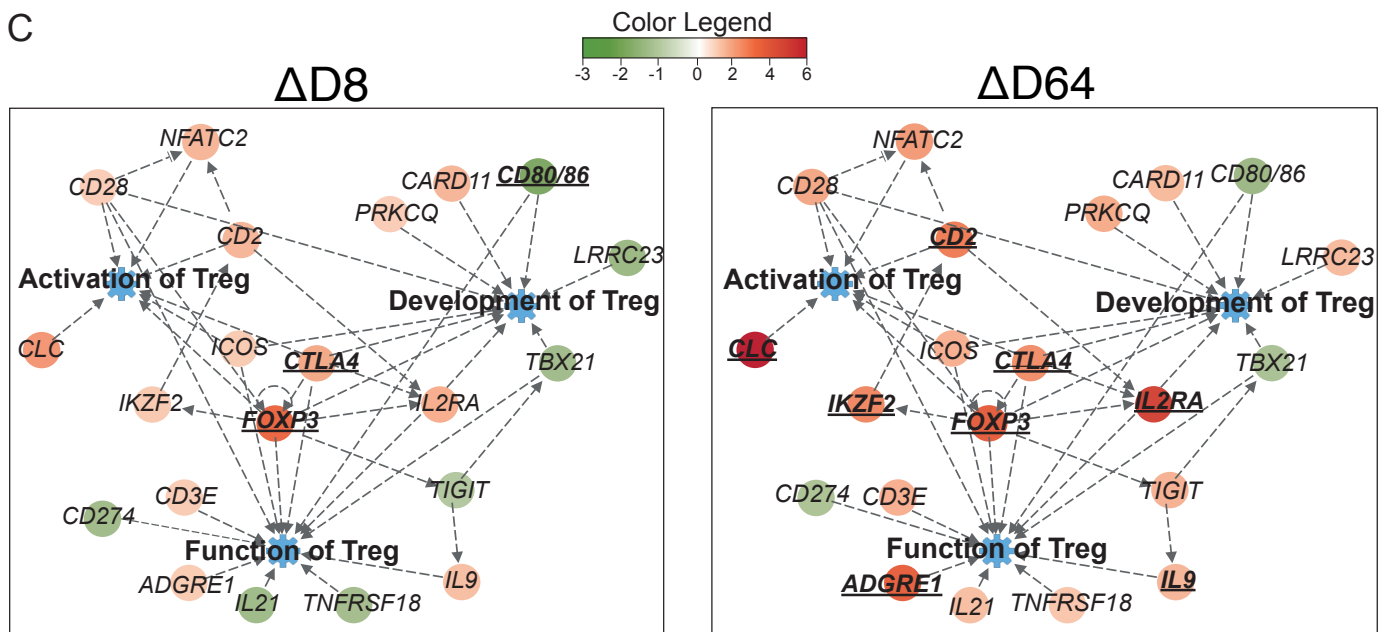
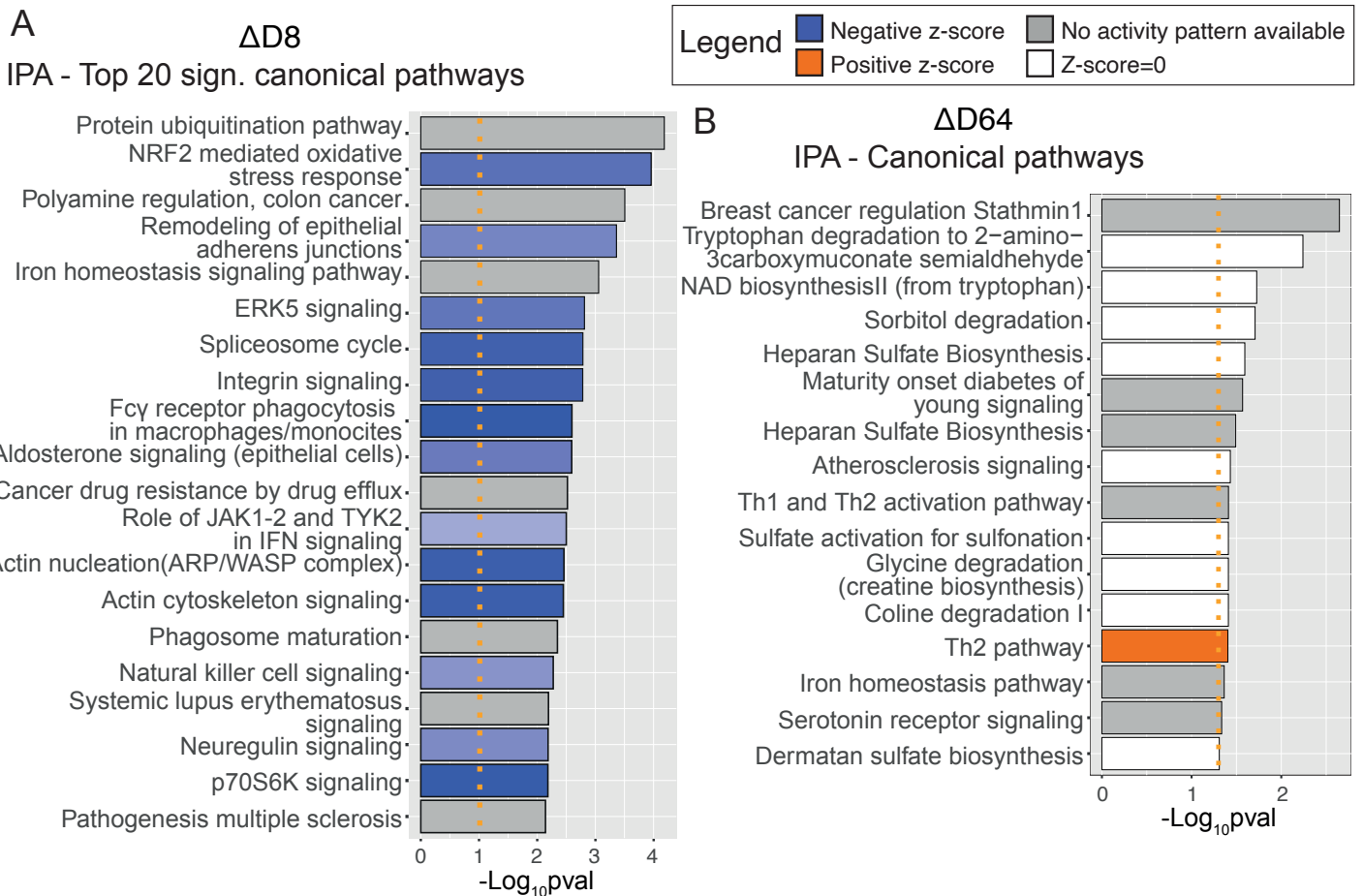


# Figure 4



Downloaded from https://academic.oup.com/braincomms/advance-article/doi/10.1093/braincomms/fcab14/6311265 by guest on 06 July 2021

# Figure 5

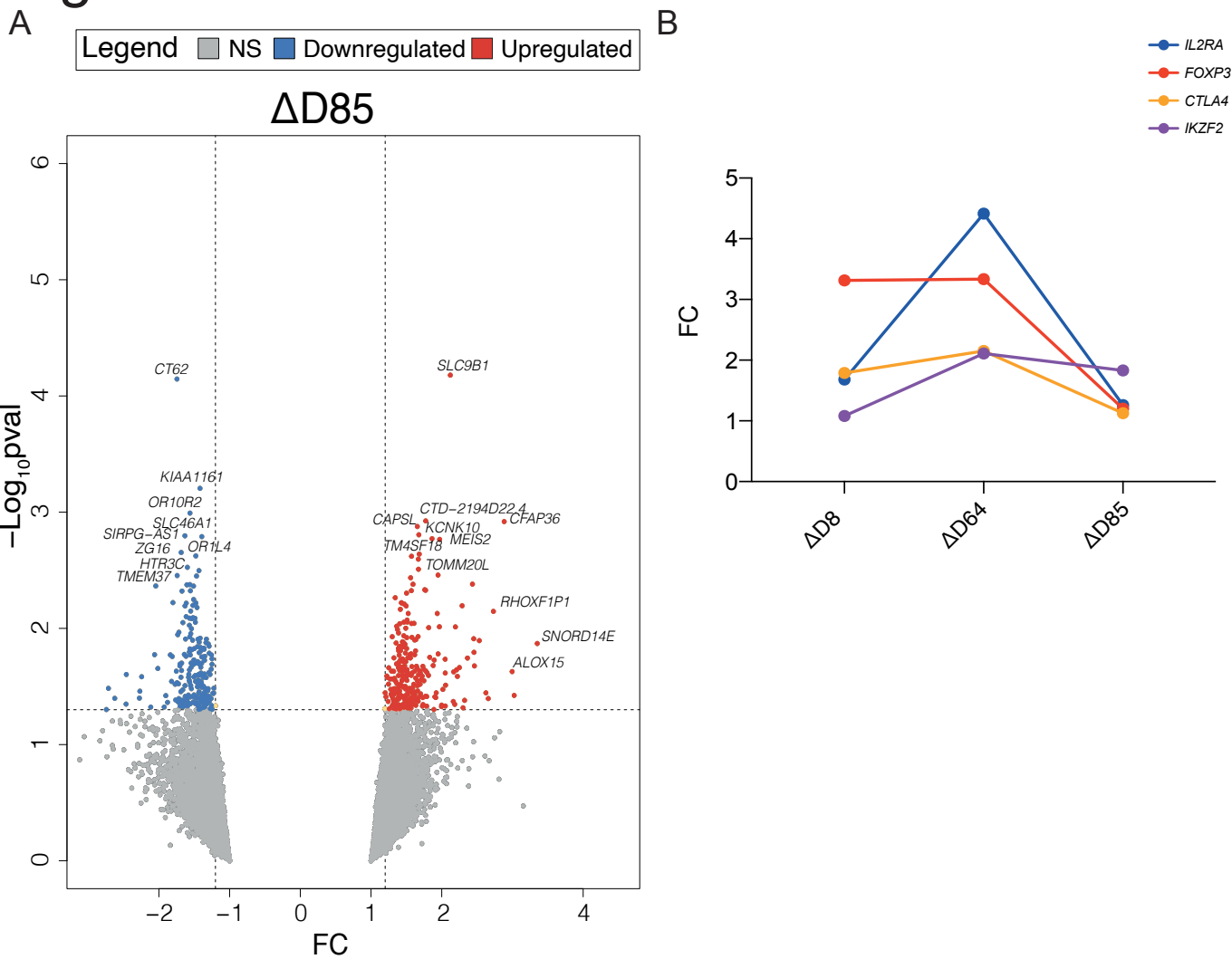
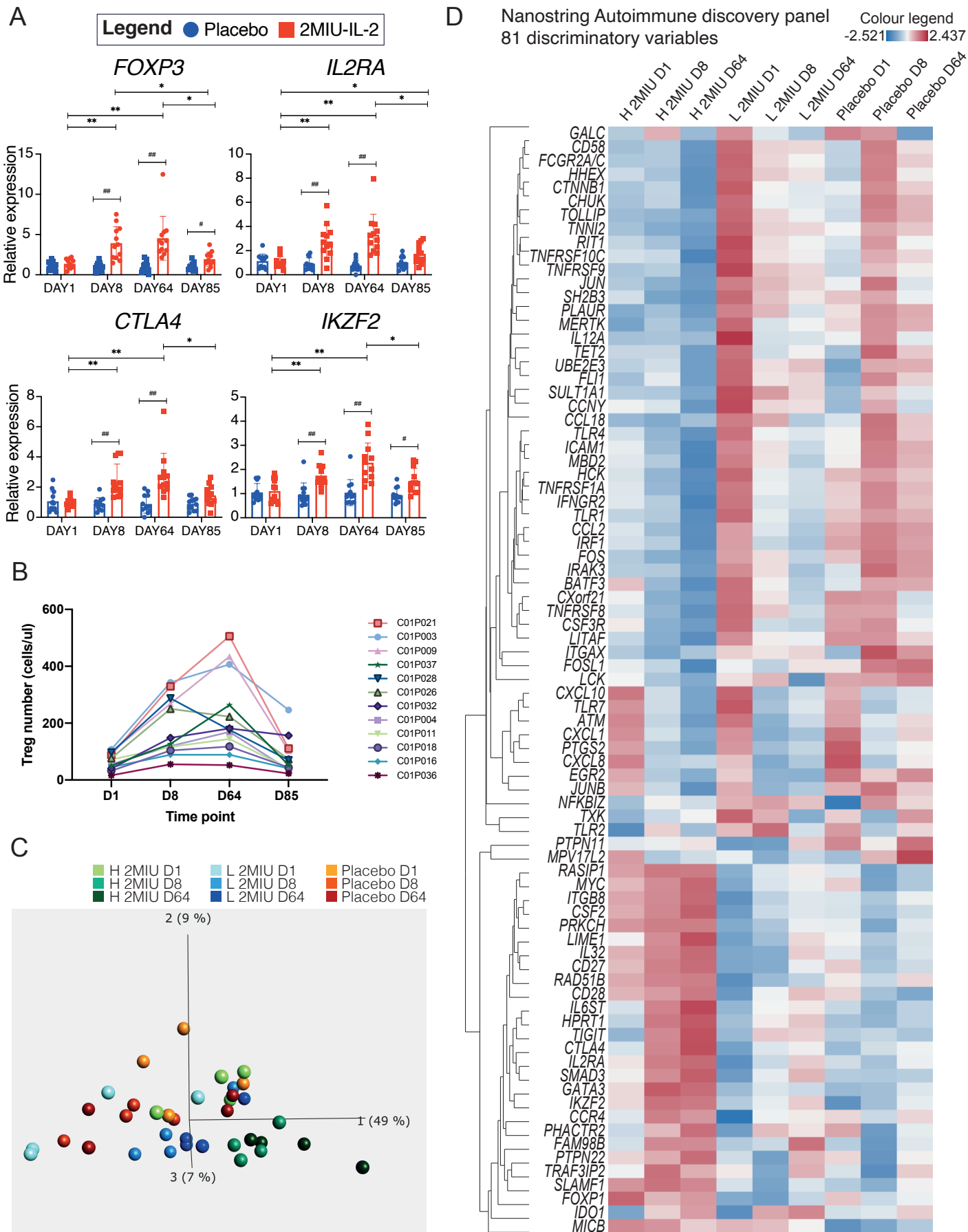
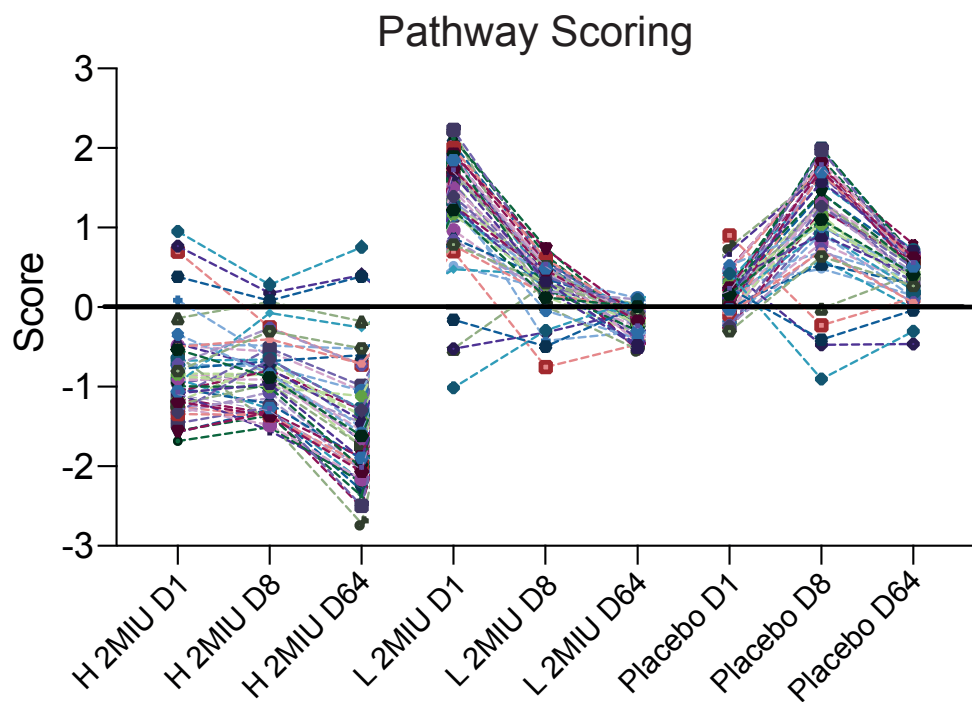


# Figure 6



Downloaded from <https://academic.oup.com/braincomms/advance-article/doi/10.1093/braincomms/fcab141/6311265> by guest on 06 July 2021

# Figure 7

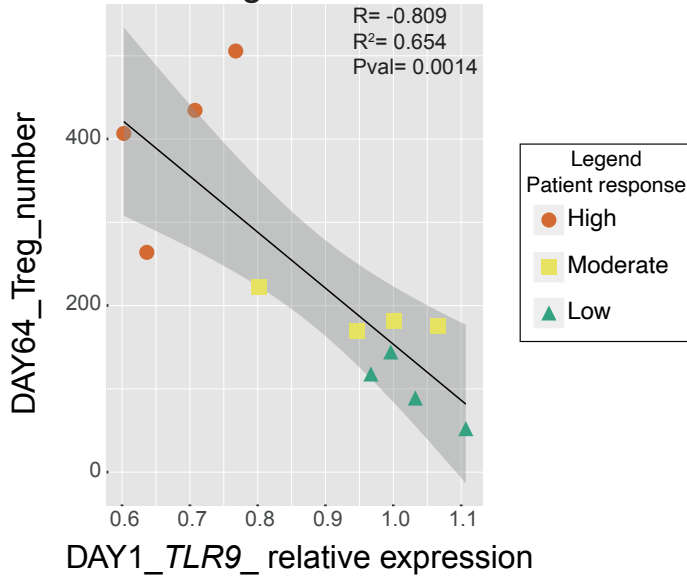


## Legend

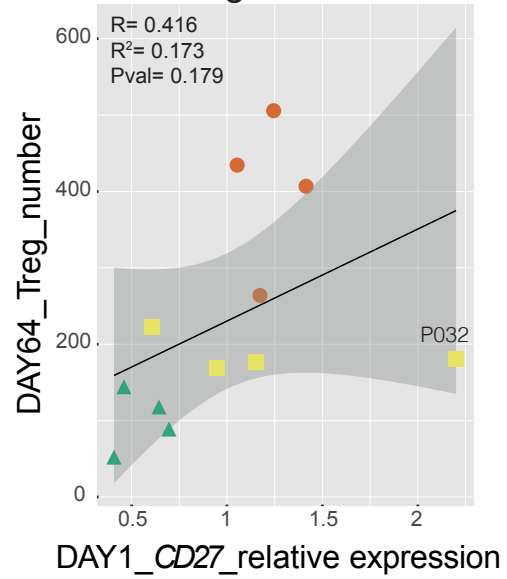
- |   |   |
|---|---|
| Antigen processing and presentation                     | MAPK signaling pathway                    |
| B cell receptor signaling pathway                       | Measles                                   |
| Cell adhesion molecules (CAMs)                          | Metabolism                                |
| Cell growth and death                                   | MicroRNAs in cancer                       |
| Cellular community                                      | NF-kappa B signaling pathway              |
| Chemokine signaling pathway                             | Natural killer cell mediated cytotoxicity |
| Choline metabolism in cancer                            | Nervous system                            |
| Complement and coagulation cascades                     | Neuroactive ligand-receptor interaction   |
| Development   | Neurodegenerative diseases                |
| Digestive system  | PI3K-Akt signaling pathway                |
| Endocrine and metabolic diseases                        | Pathways in cancer                        |
| Endocrine system  | Pertussis                                 |
| Epstein-Barr virus infection                            | Phosphatidylinositol signaling system     |
| Epithelial cell signaling in <i>H. pylori</i> infection | Proteoglycans in cancer                   |
| Fc epsilon RI signaling pathway                         | RIG-I-like receptor signaling pathway     |
| Genetic Information Processing                          | Rap1 signaling pathway                    |
| HTLV-I infection  | Ras signaling pathway                     |
| Hematopoietic cell lineage                              | Regulation of actin cytoskeleton          |
| Herpes simplex infection                                | Sensory system                            |
| Infectious diseases.CL. Parasitic                       | TGF-beta signaling pathway                |
| Inflammatory bowel disease (IBD)                        | TNF signaling pathway                     |
| Influenza A   | Toll-like receptor signaling pathway      |
| Intestinal immune network for IgA production            | Transcriptional misregulation in cancer   |
| Jak-STAT signaling pathway                              | Transport and catabolism                  |
| Leukocyte transendothelial migration                    | Tuberculosis                              |

# Figure 8

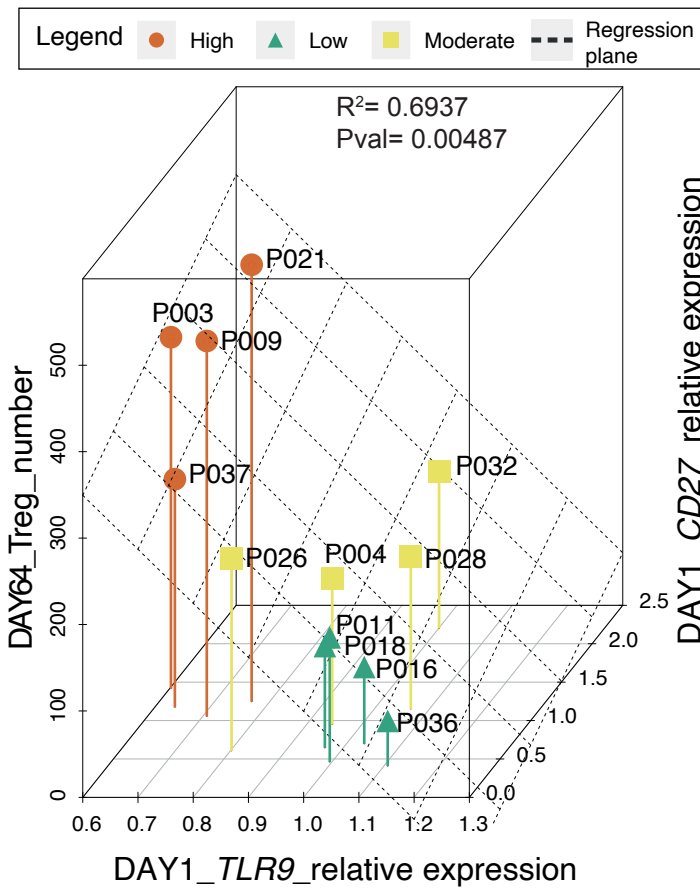
**A Linear Regression Model 1**



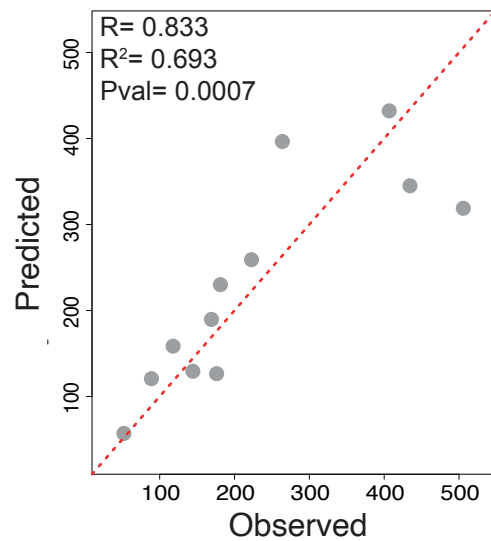
**B Linear Regression Model 2**



**C Multiple Linear Regression Model**

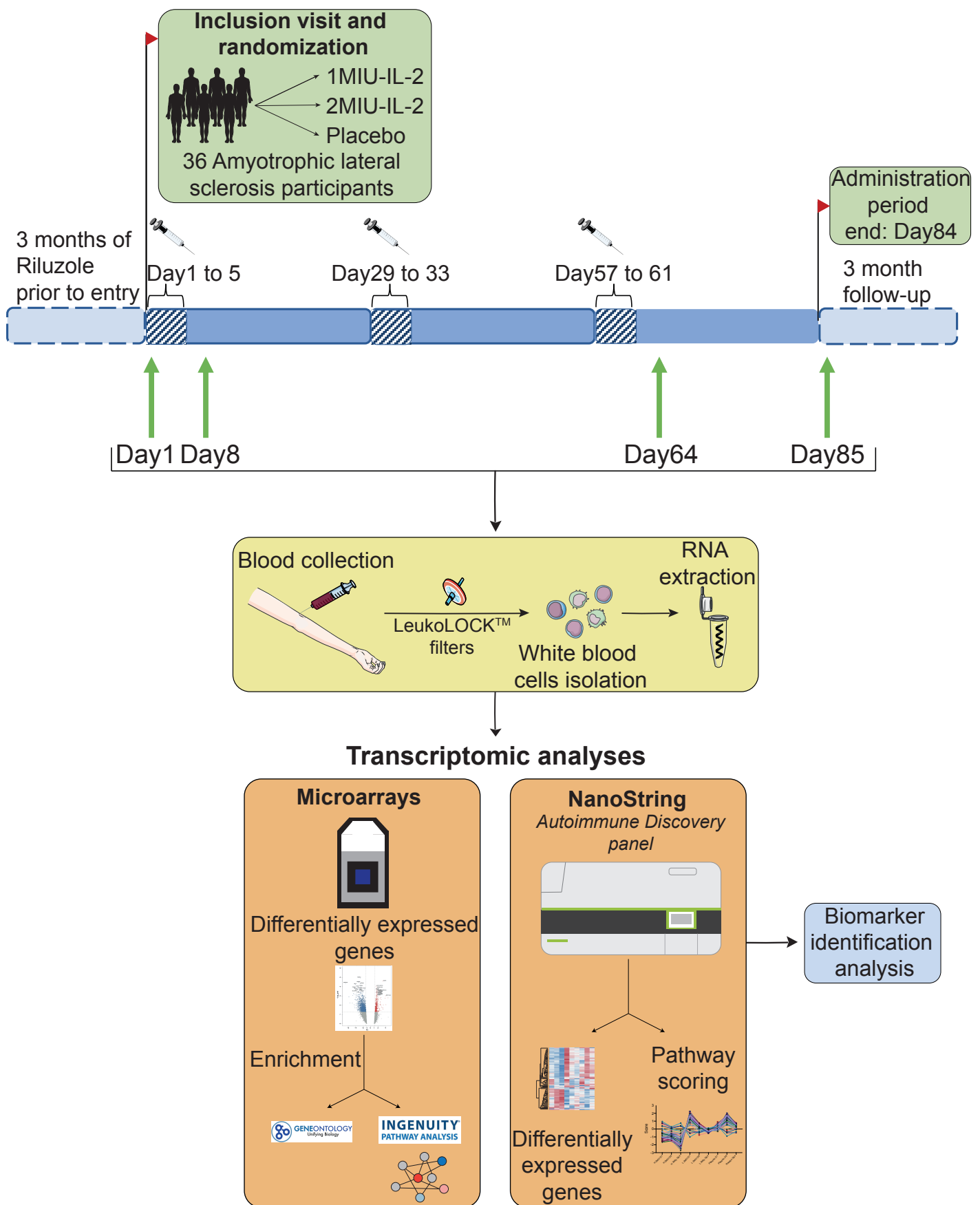


**D**



1  
2  
3 Amyotrophic lateral sclerosis patients included in the IMODALS clinical trial (NCT02059759)  
4 were transcriptionally profiled to assess longitudinal blood expression changes. Low-dose-  
5 interleukin-2 was shown to promote dose and time-dependent Treg-marker upregulation.  
6 However, inter-individual variations were reported in the magnitude of Treg expansion and  
7 a two-biomarker model to predict target-engagement was proposed.  
8  
9  
10  
11  
12  
13  
14  
15  
16  
17  
18  
19  
20  
21  
22  
23  
24  
25  
26  
27  
28  
29  
30  
31  
32  
33  
34  
35  
36  
37  
38  
39  
40  
41  
42  
43  
44  
45  
46  
47  
48  
49  
50  
51  
52  
53  
54  
55  
56  
57  
58  
59  
60

# IMODALS clinical trial



Downloaded from https://academic.oup.com/braincomms/advance-article/doi/10.1093/braincomms/fcab141/6311265 by guest on 06 July 2021